

The zebrafish mutant *dreammist* implicates sodium homeostasis in sleep regulation

Reviewed Preprint

Revised by authors after peer review.

About eLife's process

Reviewed preprint version 2

July 17, 2023 (this version)

Reviewed preprint version 1


May 9, 2023

Sent for peer review

March 14, 2023

Posted to bioRxiv

March 5, 2023

Ida L. Barlow, Eirinn Mackay, Emily Wheeler, Aimee Goel, Sumi Lim, Steve Zimmerman, Ian Woods, David A. Prober, Jason Rihel 

Department of Cell and Developmental Biology, University College London, UK; • MRC London Institute for Medical Sciences, Imperial College London, UK • Sainsbury Wellcome Centre for Neural Circuits and Behaviour, University College London, UK • MRC centre for Reproductive Health, University of Edinburgh, UK • Department of Molecular and Cellular Biology, Harvard University, USA • Ithaca College, New York, USA • Division of Biology and Biological Engineering, California Institute of Technology, Pasadena, USA

 https://en.wikipedia.org/wiki/Open_access

 <https://creativecommons.org/licenses/by/4.0/>

Abstract

Sleep is a nearly universal feature of animal behaviour, yet many of the molecular, genetic, and neuronal substrates that orchestrate sleep/wake transitions lie undiscovered. Employing a viral insertion sleep screen in larval zebrafish, we identified a novel gene, *dreammist* (*dmist*), whose loss results in behavioural hyperactivity and reduced sleep at night. The neuronally expressed *dmist* gene is conserved across vertebrates and encodes a small single-pass transmembrane protein that is structurally similar to the Na⁺,K⁺-ATPase regulator, FXYD1/Phospholemman. Disruption of either *fxyd1* or *atp1a3a*, a Na⁺,K⁺-ATPase alpha-3 subunit associated with several heritable movement disorders in humans, led to decreased night-time sleep. Since *atp1a3a* and *dmist* mutants have elevated intracellular Na⁺ levels and non-additive effects on sleep amount at night, we propose that Dmist-dependent enhancement of Na⁺ pump function modulates neuronal excitability to maintain normal sleep behaviour.

Significance statement

Sleep is an essential behavioral state, but the genes that regulate sleep and wake states are still being uncovered. A viral insertion screen in zebrafish identified a novel sleep mutant called *dreammist*, in which a small, highly-conserved transmembrane protein is disrupted. The discovery of *dreammist* highlights the importance of a class of small transmembrane-protein modulators of the sodium pump in setting appropriate sleep duration.

eLife assessment:

This study offers new **fundamental** information on a role for the sodium/potassium pump in sleep regulation. Elegant methods were used to provide **compelling** evidence supporting the claim. The work will be of interest to sleep researchers in zebrafish as well as in other species for future investigation.

Introduction

The ability of animals to switch between behaviourally alert and quiescent states is conserved across the animal kingdom (Cirelli, 2009 [↗](#); Joiner, 2016 [↗](#)). Fundamental processes that govern the regulation of sleep-like states are shared across species, such as the roles of circadian and homeostatic cues in regulating the time and amount of sleep, stereotyped postures, heightened arousal thresholds, and the rapid reversibility to a more alert state (Joiner, 2016 [↗](#)). The near ubiquity of sleep implies that it serves ancient functions and is subject to conserved regulatory processes. However, many key molecular components that modulate sleep and wake states remain undiscovered.

Over the past two decades, investigations into sleep and arousal states of genetically tractable model organisms, such as *Drosophila melanogaster*, *C. elegans*, and *Danio rerio* (zebrafish) have uncovered novel molecular and neuronal components of sleep regulation through gain- and loss-of-function genetic screens (reviewed in Barlow and Rihel, 2017 [↗](#); Sehgal and Mignot, 2011 [↗](#)). The power of screening approaches is perhaps best exemplified by the first forward genetic sleep screen, which identified the potassium channel *shaker* as a critical sleep regulator in *Drosophila* (Cirelli et al., 2005 [↗](#)). This result continues to have a lasting impact on the field, as not only did subsequent sleep screening efforts uncover the novel Shaker regulator *sleepless*, (Koh et al., 2009 [↗](#)), but investigations into Shaker's beta subunit Hyperkinetic ultimately revealed a critical role for this redox sensor linking metabolic function to sleep (Bushey et al., 2007 [↗](#); Kempf et al., 2019 [↗](#)).

Disparate screening strategies across model organisms continue to unveil novel sleep modulators in both invertebrate and vertebrate model systems. For example, the roles of RFamide receptor DMSR-1 in stress-induced sleep in *C. elegans* (Iannacone et al., 2017 [↗](#)) and SIK3 kinase in modulating sleep homeostasis in mice (Funato et al., 2016 [↗](#)) were identified in genetic screens. Moreover, a gain of function screening strategy in *Drosophila* revealed the novel sleep and immune regulator, *nemuri* (Toda et al., 2019 [↗](#)), and a zebrafish overexpression screen uncovered the secreted neuropeptides neuromedin U and neuropeptide Y, which decrease and increase sleep, respectively (Chiu et al., 2016 [↗](#); Singh et al., 2017 [↗](#)). The success of screening strategies in revealing novel sleep-wake regulatory genes suggests that more sleep signals likely remain to be discovered.

One of the lessons from these genetic screens is that many of the uncovered genes play conserved roles across species. For example, Shaker also regulates mammalian sleep (Douglas et al., 2007 [↗](#)) and RFamides induce sleep in worms, flies, and vertebrates (Lee et al., 2017 [↗](#); Lenz et al., 2015 [↗](#)). Nevertheless, not every invertebrate sleep-regulatory gene has a clear vertebrate homolog, while some human sleep/wake regulators, such as the narcolepsy- associated neuropeptide hypocretin/orexin (Chemelli et al., 1999 [↗](#); Lin et al., 1999 [↗](#); Peyron et al., 2000 [↗](#); Sakurai, 2013 [↗](#)), lack invertebrate orthologs. Therefore, genetic sleep screens in vertebrates are likely to provide added value in uncovering additional regulatory components required to control the initiation and amount of sleep in humans.

While sleep screening in mammals is feasible (Funato et al., 2016), it remains an expensive and technically challenging endeavour. With its genetic tractability, availability of high-throughput sleep assays (Rihel and Schier, 2013), and conserved sleep genetics, such as the hypocretin, melatonin, locus coeruleus, and raphe systems (Gandhi et al., 2015; Singh et al., 2015; Oikonomou et al., 2019; Prober et al., 2006), the larval zebrafish is an attractive vertebrate system for sleep screens. We took advantage of a collection of zebrafish lines that harbour viral insertions in >3500 genes (Varshney et al., 2013) to perform a targeted genetic screen. We identified a short-sleeping mutant, *dreammist*, with a disrupted novel, highly conserved vertebrate gene that encodes a small single pass transmembrane protein. Sequence and structural homology to the Na⁺/K⁺ pump regulator FXD1/Phospholemman suggests that Dreammist is a neuronal-expressed member of a class of sodium pump modulators that is important for regulating sleep-wake behaviour.

Results

Reverse genetic screen identifies *dreammist*, a mutant with decreased sleep

We used the ‘Zenemark’ viral-insertion based zebrafish gene knock-out resource (Varshney et al., 2013) to perform a reverse genetic screen to identify novel vertebrate sleep genes. This screening strategy offers several advantages compared to traditional chemical mutagenesis-based forward genetic screening approaches. First, unlike chemical mutagenesis, which introduces mutations randomly, viral insertions tend to target the 5’ end of genes, typically causing genetic loss of function (Sivasubbu et al., 2007). Second, because the virus sequence is known, it is straightforward to map and identify the causative gene in mutant animals. Finally, since viral insertions in the Zenemark collection are already mapped and sequenced, animals harbouring insertions within specific gene classes can be selected for testing (Figure S1A). This allowed us to prioritise screening of genes encoding protein classes that are often linked to behaviour, such as G-protein coupled receptors, neuropeptide ligands, ion channels, and transporters (Supplemental Data 1).

For screening, we identified zebrafish sperm samples from the Zenemark collection (Varshney et al., 2013) that harboured viral insertions in genes of interest and used these samples for *in vitro* fertilization and the establishment of F2 families, which we were able to obtain for 26 lines. For each viral insertion line, clutches from heterozygous F2 in-crosses were raised to 5 days post-fertilisation (dpf) and tracked using videography (Figure S1A) to quantify the number and duration of sleep bouts (defined in zebrafish larvae as inactivity lasting 1 minute or longer; Prober et al., 2006) and waking activity (time spent moving per active bout) over 48 hours. The genotypes of individual larvae were determined by PCR after behavioural tracking, with each larva assigned as wild type, heterozygous, or homozygous for a given viral insertion to assess the effect of genotype on sleep/wake behaviour. While most screened heterozygous and homozygous lines had minimal effects on sleep-wake behavioural parameters (Figure S1B–S1C), one homozygous viral insertion line, 10543/10543, had a reduction in daytime sleep (Figure S1B) and an increase in daytime waking activity (Figure S1C) relative to their wild type sibling controls. We re-named this 10543 viral insertion line *dreammist* (*dmist*).

In follow-up studies, we observed that animals homozygous for the viral insertion at this locus (*dmist^{vir/vir}*) showed a decrease in sleep during the day and a trend to sleep less at night compared to their wild-type siblings (*dmist^{+/+}*) (Figure 1A). *dmist* mutants had an almost 50% reduction in the average amount of daytime sleep (Figure 1C) due to a decrease in the number of sleep bouts (Figure 1D), whereas the sleep bout length at night was significantly reduced (Figure 1E). *dmist^{vir/vir}* larvae also exhibited significantly increased daytime waking activity, which is the locomotor activity while awake (Figure 1B, 1F). Because Zenemark lines can contain more than

one viral insertion (17.6% of lines have ≥ 2 insertions; Varshney et al 2013 [↗](#)), we outcrossed *dmist*^{vir/+} fish to wild-type fish of the AB-TL background and re-tested *dmist* mutant fish over several generations. Normalising all the behavioural parameters to *dmist*^{+/+} controls with a linear mixed effects (LME) model showed consistent sleep changes in *dmist*^{vir/vir} fish over 5 independent experiments (**Figure 1G** [↗](#)). The *dmist*^{vir/vir} larvae consistently show a more than 50% decrease in sleep during the day due to a significant reduction in the number and duration of sleep bouts, as well as a large increase in waking activity (**Figure 1G** [↗](#)). The *dmist*^{vir/vir} mutants also had a significant reduction in sleep at night compared to wild type siblings (**Figure 1G** [↗](#)). These effects on sleep and wakefulness are not due to alterations in circadian rhythms, as behavioural period length in fish that were entrained and then shifted to free-running constant dark conditions was unaffected in *dmist*^{vir/vir} compared to wild-type sibling larvae (**Figure S2A** [↗](#)-S2C).

The *dmist* gene encodes a novel, small transmembrane protein

Having identified a sleep mutant, we next sought to investigate the target gene disrupted by the viral insertion. Line 10543 (*dmist*^{vir}) was initially selected for screening due to a predicted disruption of a gene encoding a serotonin transporter (*slc6a4b*) on chromosome 5. However, mapping of the *dmist* viral insertion site by inverse-PCR and sequencing revealed that the virus was instead inserted into the intron of a small two-exon gene annotated in the Zv6 genome assembly as a long intergenic non-coding RNA (lincRNA; gene transcript ENSDART00000148146, gene name *si:dkey234h16.7*), which lies approximately 6 kilobases (kb) downstream of the *slc6a4b* gene in zebrafish. At least part of this region is syntenic across vertebrates, with a small two-exon gene identified adjacent to the genes *ankrd13a* and *GIT* in several vertebrates, including human and mouse (**Figure 2A** [↗](#)). Amplifying both 5' and 3' ends of zebrafish *si:dkey234h16.7* and mouse E13.5 1500011B03-001 transcripts with Rapid Amplification of cDNA ends (RACE) confirmed the annotated zebrafish and mouse transcripts and identified two variants with 3' untranslated regions (3'UTR) of different lengths in zebrafish (**Figure S3B** [↗](#)). To test whether the viral insertion in *dmist*^{vir/vir} disrupts expression of *si:dkey234h16.7* or neighbouring genes, we performed quantitative analysis of gene transcript levels in wild type and mutant *dmist* larvae by RT-qPCR. This revealed that the *dmist* viral insertion caused a more than 70% reduction in the expression of *si:dkey234h16.7* while the expression of the most proximal 5' or 3' flanking genes, *slc6a4b_Dr* and *ankrd13a_Dr*, were unaffected (**Figure 2B** [↗](#) and S3A). Since this reduced expression is most consistent with *si:dkey234h16.7* being the causal lesion of the *dmist* mutant sleep phenotype, we renamed this gene *dreammist* (*dmist*).

Computational predictions indicated that the *dmist* transcripts contain a small open reading frame (ORF) encoding a protein of 70 amino acids (aa) (**Figure 2C** [↗](#)). Querying the human and vertebrate protein databases by BLASTp using the C-terminal protein sequence of Dmist identified orthologs in most vertebrate clades, including other species of teleost fish, birds, amphibians, and mammals (**Figure 2A** [↗](#), C). All identified orthologs encoded predicted proteins with an N-terminal signal peptide sequence and a C-terminal transmembrane domain (**Figure 2C** [↗](#)). The peptide sequence identity across orthologs ranged from 38 to 84%, with three peptide motifs (QNLV, CVYKP, RRR) showing high conservation across all vertebrates, and high similarity for many additional residues (**Figure 2C** [↗](#), **Figure S3D** [↗](#)). Additional searches by tBLASTn failed to identify any non-vertebrate *dmist* orthologs. In summary, we found that the *dreammist* gene, the expression of which is disrupted in *dmist*^{vir/vir} fish with sleep phenotypes, encodes a protein of uncharacterized function that is highly conserved across vertebrates at both the genomic and molecular levels.

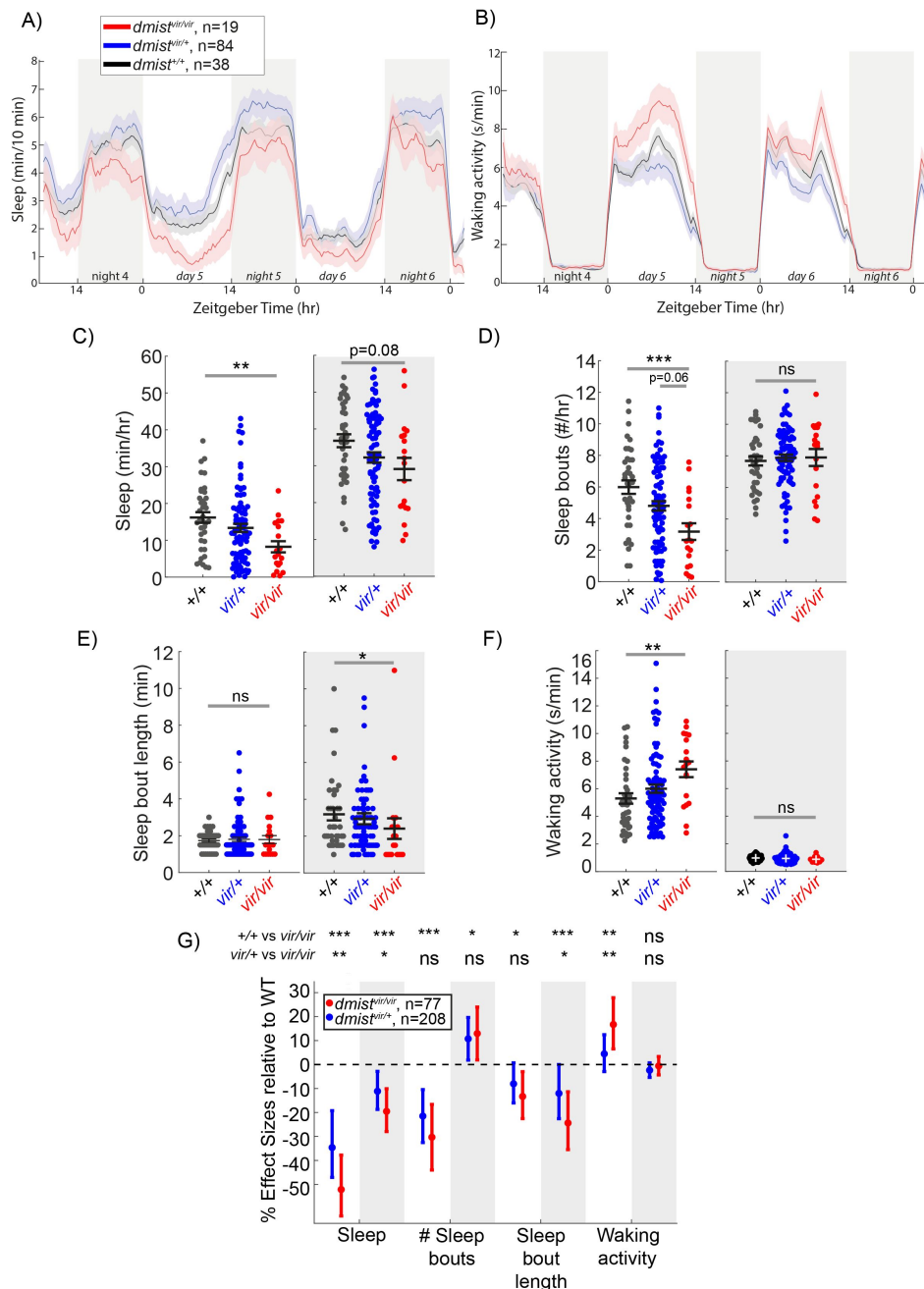


Figure 1.

A viral insertion mini-screen identifies a short-sleeping mutant, *dreammist*.

A-B) Mean± SEM sleep (A) and waking activity (B) of progeny from *dmist*^{vir/+} in-cross from original screen. White blocks show day (lights on) and grey blocks show night (lights off). Data is combined from 2 independent experiments. n indicates the number of animals.

C-F) Analysis of sleep/wake architecture for the data shown in (A, B). C) Quantification of total sleep across two days and nights shows decreased day and night sleep in *dmist*^{vir/vir}. Analysis of sleep architecture reveals fewer sleep bouts during the day (D) and shorter sleep bouts at night (E) in *dmist*^{vir/vir} compared with sibling controls. F) Daytime waking activity is also increased in *dmist*^{vir/vir}. The black lines show the mean ± SEM, except in E, which labels the median ± SEM. *p<0.05, **p<0.01, ***p<0.001; ns p>0.05; one-way ANOVA, Tukey's post hoc test.

G) Combining 5 independent experiments using a linear mixed effects model with genotype as a fixed effect and experiment as a random effect reveals *dmist*^{vir/vir} larvae have decreased total sleep and changes to sleep architecture during both the day and night compared to *dmist*^{+/+} siblings. Plotted are the genotype effect sizes (95% confidence interval) for each parameter relative to wild type. Shading indicates day (white) and night (grey). P-values are assigned by an F-test on the fixed effects coefficients from the linear mixed effects model. *p<0.05, **p<0.01, ***p<0.001, ns p>0.05. n indicates the number of animals.

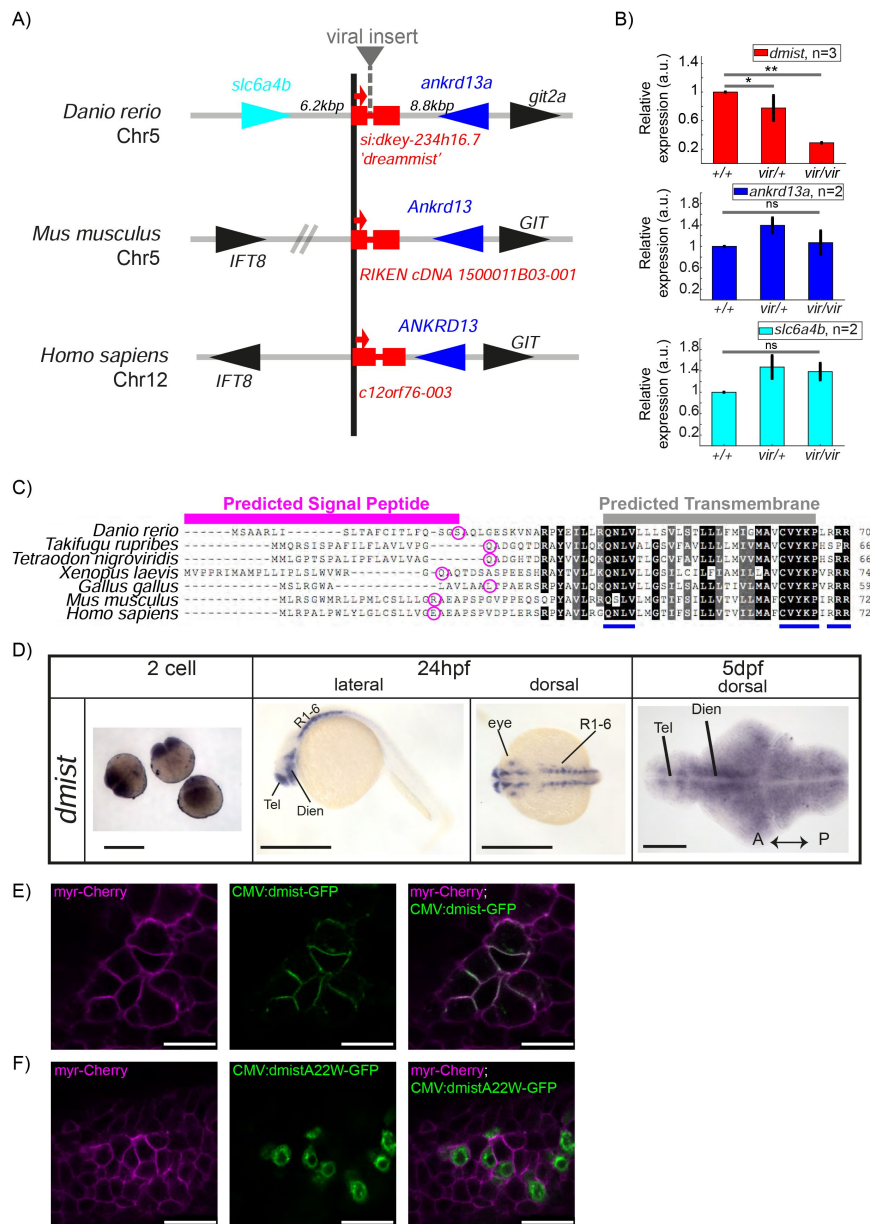


Figure 2.

***dmist* encodes a conserved vertebrate single pass transmembrane protein.**

A) *dmist* mutants harbour a viral insertion in the 1st intron of *si:key-234h16.7*. *dmist* is syntenic with *Ankrd13* and *GIT* orthologs in mouse, human, and zebrafish.

B) RT-qPCR of *dmist* (red) show reduced expression of *dmist* and not the 5' and 3' flanking zebrafish genes, *slc6a4b* (cyan) and *ankrd13a* (blue), in *dmist*^{vir/vir} larvae compared to *dmist*^{vir/+} and *dmist*^{+/+} siblings. **p<0.01, *p<0.05; ns p>0.05; one-way ANOVA, Tukey's post-hoc test. Data shows mean ± SEM normalized to the wild type mean.

C) *dmist*_{Dr} contains an open reading frame encoding a 70 amino acid protein that is conserved across vertebrates. All identified homologues have a predicted signal peptide sequence (magenta line), signal peptide cleavage site (magenta circle), and predicted transmembrane domain (grey), with additional highly conserved C-terminal motifs (blue lines). Identical amino acids in all species are shown in black; similar amino acids (80-99% conserved across species) are shown in grey.

D) *In situ* hybridisation using a *dmist* antisense probe reveals *dmist* is maternally deposited as it is detected at the 2-cell stage. At 24 hpf expression is restricted to regions containing neuronal precursors, and at 5 dpf expression is widespread throughout the brain. Tel, telencephalon; Dien, diencephalon; R1-6, rhombomeres 1-6; A, anterior; P, posterior. Scale bars= 0.5 mm (2 cell and 24 hpf), 0.1 mm (5 dpf).

E-F) Representative confocal image of 90% epiboly embryo co-injected at the 1-cell stage with mRNA encoding membrane-RFP (magenta) and a plasmid encoding either C-terminal tagged Dmist-GFP (E, green) or DmistA22W-GFP (F, green). Scale bar= 25 μm.

Genetic molecular analysis of *dmist* expression in zebrafish and mouse

Because the viral insertion disrupts *dmist* throughout the animal's lifetime, we examined both the developmental and spatial expression of *dmist* to assess when and where its function may be required for normal sleep. Using the full-length transcript as a probe (**Figure S3B** [↗](#)), we performed *in situ* hybridization across embryonic and larval zebrafish development. Maternally deposited *dmist* was detected in early embryos (2-cell stage) prior to the maternal to zygotic transition (Giraldez et al., 2006 [↗](#)) (**Figure 2D** [↗](#)). Consistent with maternal deposition of *dmist* transcripts, inspection of the 3' end of the *dmist* gene revealed a cytoplasmic polyadenylation element ("TTTTTAT"; Supplemental Information 2) that is required for zygotic translation of maternal transcripts (Villalba et al., 2011 [↗](#)). At 24 hpf, transcripts were detected in regions that form the embryonic brain, such as ventral telencephalon, diencephalon and cerebellum, and in the developing eye (**Figure 2D** [↗](#), S3C). By 5 dpf, *dmist* transcripts were detected throughout the brain (**Figure 2D** [↗](#)). To test whether *dmist* transcripts are under circadian regulation, we performed RT-qPCR in fish that were entrained and then shifted to free-running constant dark conditions. In contrast with the robust 24-hr rhythmic transcription of the circadian clock gene *per1*, we did not detect any changes in *dmist* expression throughout the 24 hour circadian cycle (**Figure S2D** [↗](#)).

Consistent with brain expression in larval zebrafish, we identified the expression of *Dmist_Mm* in a published RNAseq dataset of six isolated cell types from mouse cortex (Zhang et al., 2014 [↗](#)). We confirmed that *Dmist_Mm* is specifically enriched in neurons by hierarchical clustering of all 16,991 expressed transcripts across all six cell types, which demonstrated that *Dmist_Mm* co-clusters with neuronal genes (**Figure S3E** [↗](#)). Pearson correlation of *Dmist_Mm* with canonical markers for the six cell types showed that *Dmist_Mm* expression is highly correlated with other neuronal genes but not genes associated with microglia, oligodendrocytes, or endothelia. This result indicates that *dmist* is specifically expressed in neurons in both zebrafish and mouse (**Figure S3F** [↗](#)).

Dmist localises to the plasma membrane

Although the *dmist* gene encodes a conserved ORF with a predicted signal peptide sequence and transmembrane domain (**Figure 2C** [↗](#); **Figure S3G** [↗](#)-I), we wanted to confirm this small peptide can localise to the membrane and if so, on which cellular compartments. To test these computational predictions, we transiently co-expressed GFP-tagged Dmist (C-terminal fusion) with a marker for the plasma membrane (myr-Cherry) in zebrafish embryos. Imaging at 90% epiboly revealed Dmist-GFP localised to the plasma membrane (**Figure 2E** [↗](#)). Conversely, introducing a point mutation into Dmist's signal peptide cleavage site (DmistA22W-GFP) prevented Dmist from trafficking to the plasma membrane, with likely retention in the endoplasmic reticulum (**Figure 2F** [↗](#)). Together, these data indicate that Dmist localises to the plasma membrane despite its small size, as computationally predicted.

CRISPR/Cas9 generated *dmist*ⁱ⁸ mutant exhibits decreased night-time sleep

dmist expression was reduced by 70% in the viral insertion line, suggesting that *dmist*^{vir} is a hypomorphic allele. To confirm that the sleep phenotypes observed in *dmist*^{vir/vir} animals are due to the loss of Dmist function, we used CRISPR/Cas9 to create an independent *dmist* loss of function allele. We generated a zebrafish line in which the *dmist* gene contains an 8 bp insertion that causes a frameshift and early stop codon (*dmist*ⁱ⁸, **Figure 3A** [↗](#)). The *dmist*ⁱ⁸ allele is predicted to encode a truncated protein lacking the complete signal peptide sequence and transmembrane

domain (**Figure 3B** [↗](#)), indicating this is likely a null allele. RT-qPCR showed that *dmist* transcript levels were 60% lower in *dmist^{i8/i8}* fish compared to wild type siblings, consistent with nonsense-mediated decay (**Figure S4A** [↗](#), B) (Wittkopp et al., 2009 [↗](#)).

We next assessed the sleep and activity patterns of *dmist^{i8/i8}* fish. As seen in exemplar individual tracking experiments, *dmist^{i8/i8}* larvae sleep less at night due to fewer sleep bouts and also show an increase in waking activity relative to wild type and heterozygous mutant siblings (**Figure 3C-H** [↗](#)). This significant night-time reduction in sleep and increase in hyperactivity is also apparent when combining 5 independent experiments with a linear mixed effects (LME) model to normalize behaviour across datasets (**Figure 3I** [↗](#)). Although *dmist^{vir/vir}* larvae also sleep less at night (**Figure 1G** [↗](#)), the large day-time reduction in sleep observed in *dmist^{vir/vir}* larvae is absent in *dmist^{i8/i8}* animals, perhaps due to differences in genetic background that affect behaviour. Because the *dmist^{vir}* is likely a hypomorphic allele, we focused subsequent experiments on the CRISPR-generated *dmist^{i8/i8}* larvae.

To test whether the increased night-time activity of *dmist^{i8/i8}* mutants persists in older animals, we raised *dmist^{i8/i8}* mutants with their heterozygous and wild type siblings to adulthood in the same tank and tracked individual behaviour for several days on a 14:10 light:dark cycle. As in larval stages, *dmist^{i8/i8}* adults were hyperactive relative to both *dmist^{i8/+}* and *dmist^{+/+}* siblings, maintaining a higher mean speed at night (**Figure 3J-L** [↗](#)). This suggests that either Dmist affects a sleep/wake regulatory circuit during development that is permanently altered in *dmist* mutants, or that Dmist is continuously required to maintain normal levels of night-time locomotor activity.

Dmist is distantly related to the Na⁺/K⁺ pump regulator Fxyd1 (Phospholemman)

Because Dmist is a small, single pass transmembrane domain protein without any clear functional motifs and has not been functionally characterized in any species, we searched for similar peptides that might provide clues for how Dmist regulates behaviour. Using the multiple sequence alignment tool MAFFT to align the zebrafish, mouse, and human Dmist peptides (Katoh and Toh, 2010 [↗](#)) and seeding a hidden Markov model iterative search (JackHMMR) of the Uniprot database (Johnson et al., 2010 [↗](#)), we found distant homology between Dmist and Fxyd1/Phospholemman (**Figure 4A** [↗](#)), a small transmembrane domain peptide that regulates ion channels and pumps, including the Na⁺, K⁺-ATPase pump (Crambert et al., 2002 [↗](#)). Dmist and Fxyd1 share 27-34% amino acid homology, including an RRR motif at the C-terminal end, although Dmist lacks a canonical FXYP sequence (**Figure 4A** [↗](#)). In addition, computational predictions using the AlphaFold protein structure database revealed structural similarities between Dmist and Fxyd1 (Jumper et al., 2021 [↗](#)), suggesting that Dmist may belong to a class of small, single pass transmembrane ion pump regulators.

Using *In situ* hybridisation, we found that *fxyd1* is expressed in cells along the brain ventricle and choroid plexus (**Figure 4C** [↗](#)) in contrast to the neuronal expression of *dmist* (**Figure 2D** [↗](#)). Despite these different expression patterns, based on their sequence similarity we reasoned that Fxyd1 and Dmist may regulate the same molecular processes that are involved in sleep. To test this hypothesis, we used CRISPR/Cas9 to generate a 28 bp deletion in the third exon of the zebrafish *fxyd1* gene, causing a frameshift that is predicted to encode a truncated protein that lacks the FXYP, transmembrane, and C-terminal domains (**Figure 4B** [↗](#)). Contrary to a previous report based on morpholino knockdown (Chang et al., 2012 [↗](#)), *fxyd1^{Δ28/Δ28}* larvae were viable with no detectable defect in inflation of the brain ventricles. We therefore tested *fxyd1* mutant larvae for sleep phenotypes. Like *dmist* mutants, *fxyd1^{Δ28/Δ28}* larvae slept less at night (**Figure 4D-F** [↗](#)). Interestingly, this sleep loss is mainly due to shorter sleep bouts (**Figure 4F** [↗](#)), indicating that *fxyd1* mutants initiate sleep normally but do not properly maintain it, unlike *dmist* mutants, which

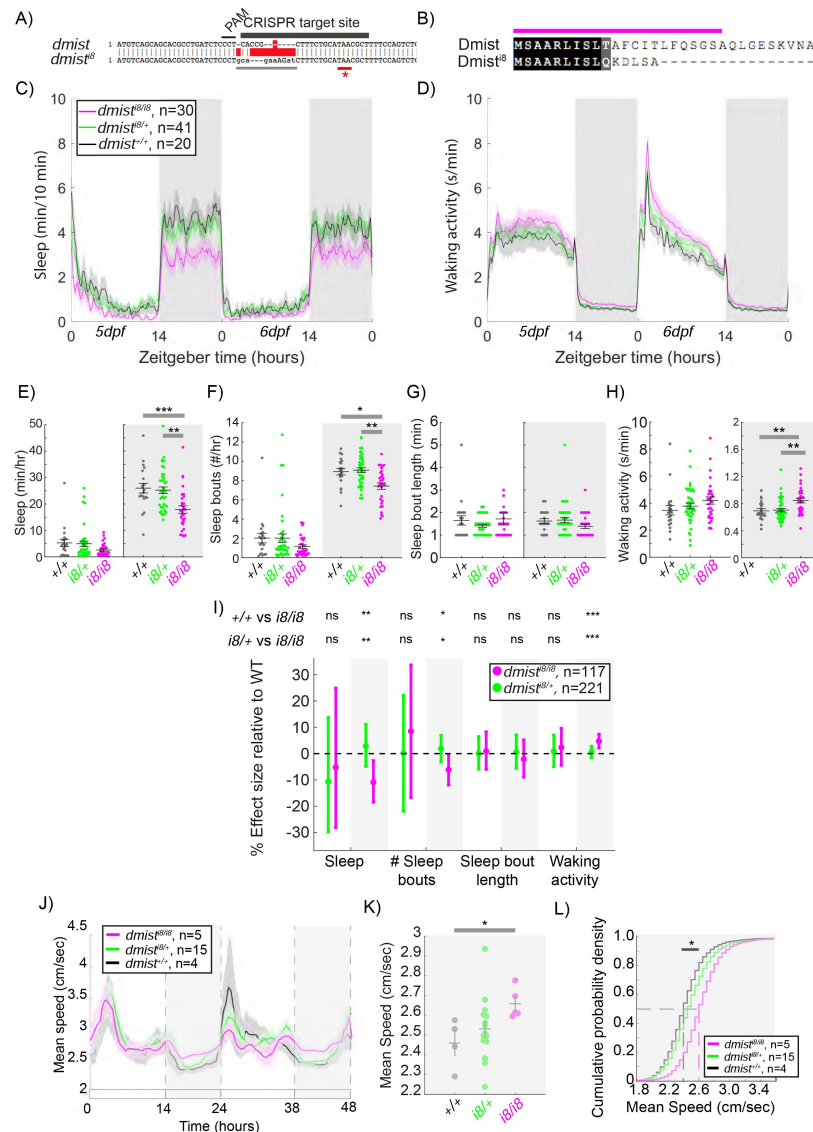


Figure 3.

CRISPR-generated *dmist* mutants sleep less and are hyperactive at night.

A) CRISPR/Cas9 targeting of the first exon of *dmist* resulted in an 8 bp insertion (*dmist*ⁱ⁸) (grey line) within the coding sequence, leading to an early stop codon (red line with *). Guide RNA target sequence and PAM sequence are shown as black bars. The sequence that is deleted in the mutant is indicated with a red bar.

B) Predicted Dmistⁱ⁸ peptide sequence lacks most of the N-terminal signal peptide sequence (magenta) and the full C-terminus.

C-D) Representative 48 hr traces of mean ± SEM sleep (C) and waking activity (D) shows decreased sleep and increased waking activity at night for *dmist*^{i8/i8} fish compared to *dmist*^{i8/+} and *dmist*^{+/+} siblings. n=number of fish.

E-H) Analysis of sleep/wake architecture of the experiment depicted in (C, D) indicates that *dmist*^{i8/i8} larvae sleep less at night (E) due to fewer sleep bouts (F). Sleep bout length is unchanged (G). Waking activity is also increased in *dmist*^{i8/i8} fish (H). The black line represents the mean ± SEM except for G, which is the median ± SEM. *p<0.05, **p<0.01, ***p<0.001; One-way ANOVA, Tukey's post hoc test.

I) Combining 5 independent experiments with a linear mixed effects model reveals *dmist*^{i8/i8} fish sleep less at night due to fewer sleep bouts and also show increased waking activity at night. Plotted are the genotype effect sizes (95% confidence interval) for each parameter relative to wild type. Shading indicates day (white) and night (grey). P-values are assigned by an F-test on the fixed effects coefficients from the linear mixed effects model. *p<0.05, **p<0.01, ***p<0.001, ns p>0.05.

J-K) (J) Adult *dmist*^{i8/i8} fish have a higher mean swim speed compared to their wild type siblings at night. Data in (J) is quantified at night in (K). (J, K) show mean ± SEM. *p<0.05, one-way ANOVA.

L) Cumulative probability distribution of all night-time swim bout speeds in adult fish. The dashed lines show the half max (0.5 probability) for each curve. *p<0.05 for *dmist*^{i8/i8} fish compared to wild type siblings; Kolmogorov-Smirnov test.

initiate fewer night-time sleep bouts, although in both cases there is consolidation of the wake state at night (**Figure 3I**, 4F). Thus, despite the non-neuronal expression of *fxyd1* in the brain, mutation of the gene most closely related to *dmist* results in a similar sleep phenotype.

The brain-wide Na⁺/K⁺ pump alpha subunit Atp1a3a regulates sleep at night

Given the similarity between *Dmist* and *Fxyd1* and their effects on night-time sleep, we hypothesized that mutations in Na⁺/K⁺ pump subunits known to interact with *Fxyd1* might also affect sleep. Consistent with this hypothesis, a low dose of the Na⁺/K⁺ pump inhibitor, ouabain, reduced night-time sleep in dose-response studies (**Figure S5A**). When applied in the late afternoon of 6 dpf, 1 μM ouabain decreased subsequent night-time sleep by 16.5% relative to controls, an effect size consistent with those observed in *dmist* mutants (**Figure 5A**, C). Night-time waking activity was also significantly increased after low-dose ouabain exposure (**Figure 5B**, D). Ouabain binds to specific sites within the first extracellular domain of Na⁺/K⁺ pump alpha subunits (Price and Lingrel, 1988), and species-specific changes to these sites confers species-specific ouabain resistance, as in the case of two naturally occurring amino acid substitutions present in the Atp1a1 subunit of mice (Dostanic et al., 2004). Alignment of the ouabain sensitive region of zebrafish and mouse Na⁺/K⁺ pump alpha subunits revealed that zebrafish Atp1a1a lacks the conserved Glutamine at position 121 (**Figure 5E**), suggesting that one of the other subunits with conserved ouabain-binding sites is responsible for the low dose ouabain sleep effects. We focused on the Na⁺/K⁺ pump alpha-3 subunit (Atp1a3), as this has been shown to directly interact with *Fxyd1* in mammalian brain tissue (Feschenko et al., 2003). Murine *Dmist* expression also correlates well with the *Atp1a3* distribution across 5 brain cell types in mouse (Pearson correlation coefficient = 0.63), which has the strongest correlation score with neuronal markers (**Figure S5B** compared to **Figure S3F**). In contrast, zebrafish *atp1a2a* is reportedly expressed in muscle at larval stages, while *atp1a1b* is confined to cells along the ventricle (Thisse et al., 2001).

Zebrafish have two Atp1a3 paralogs, *atp1a3a* and *atp1a3b*. Similar to *dmist*, *atp1a3a* is widely expressed in the larval zebrafish brain (**Figure 5F**, compare to **Figure 2D**). While *atp1a3b* is also expressed in the zebrafish brain, its expression is more limited to regions of the midbrain and hindbrain (**Figure S5C**). To test whether these genes are involved in regulating zebrafish sleep, we used CRISPR/Cas9 to isolate an allele of *atp1a3a* containing a 19 bp deletion and an allele of *atp1a3b* containing a 14 bp deletion. Both mutations are predicted to generate null alleles due to deletion of the start codon (**Figure 5G**, S5D). Both *atp1a3a*^{Δ19/Δ19} and *atp1a3b*^{Δ14/Δ14} mutant larvae were healthy and viable through early development, although *atp1a3b* mutant larvae were not obtained at Mendelian ratios (55 wild type [52.5 expected], 142 [105] *atp1a3b*^{+/-}, 13 [52.5] *atp1a3b*^{-/-}; p<0.0001, Chi-squared), suggesting some impact on early stages of development leading to lethality. Contrary to a previous report based on morpholino injections (Doğanli et al., 2013), neither mutant had defects in the inflation of their brain ventricles. Sleep-wake tracking experiments found that *atp1a3b*^{Δ14/Δ14} mutants were more active during the day with minimal sleep phenotypes (**Figure S5E**–G). In contrast, mutation of *atp1a3a* resulted in large effects on sleep-wake behaviour. Compared to wild type and heterozygous mutant siblings, *atp1a3a*^{Δ19/Δ19} animals were hyperactive throughout the day and night and had a large reduction in sleep at night (**Figure 5H**, I). The night-time sleep reduction was due to a reduction in the length of sleep bouts, as *atp1a3a* mutants even had a small increase in the number of sleep bouts at night (**Figure 5J**). In conclusion, loss of *atp1a3a* results in sleep loss at night, similar to treatment with the small molecule ouabain, and to *dmist* and *fxyd1* mutants. Notably, the *atp1a3a* mutant phenotype is much stronger, as might be expected if *Dmist* plays a modulatory, and Atp1a3a a more central, role in Na⁺/K⁺ pump activity.

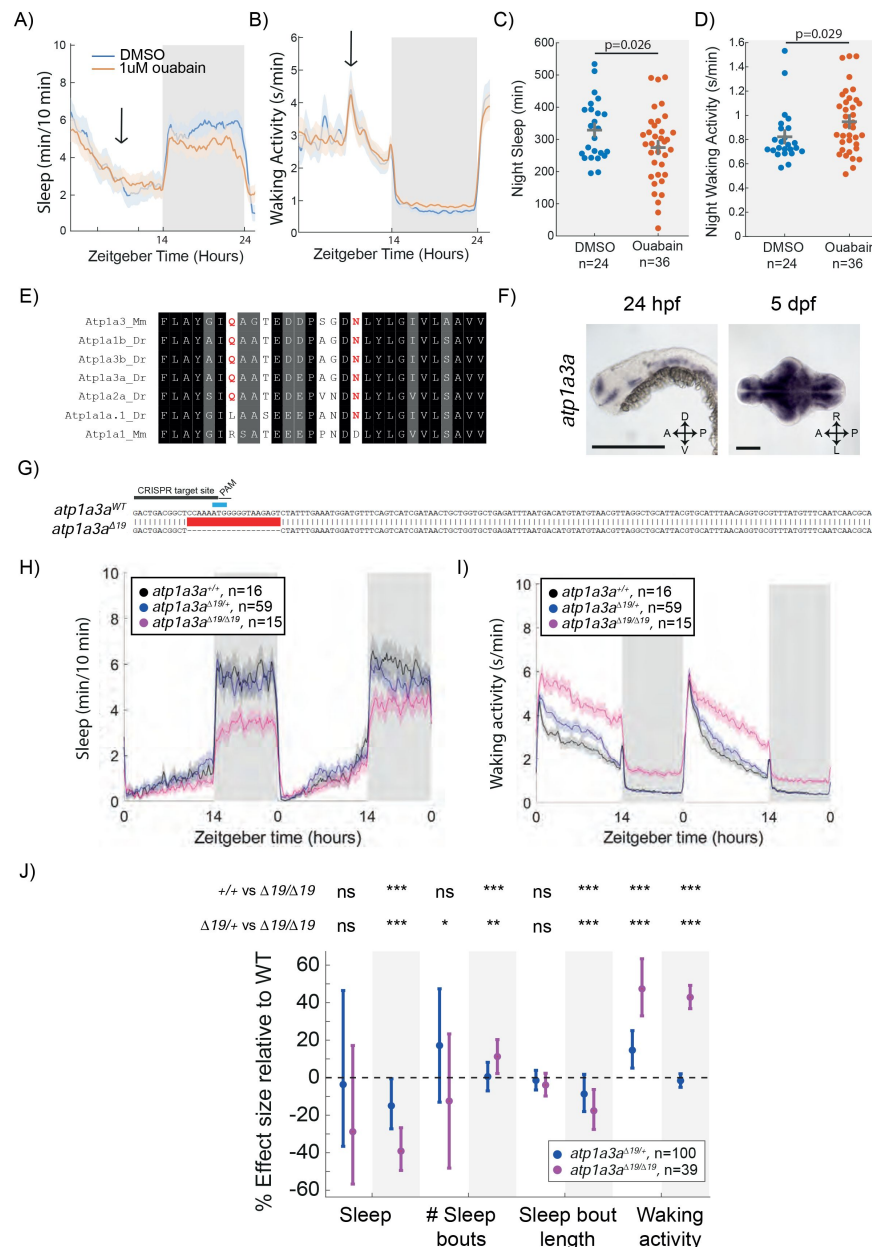


Figure 5.

Mutation of the Na⁺/K⁺ pump alpha subunit *atp1a3a* reduces sleep at night

A-B) Mean \pm SEM sleep and waking activity traces of wild type larvae following exposure to 1 μ M ouabain. Arrows indicate time the drug was added.

C-D) At night, sleep is significantly reduced and waking activity is significantly increased after ouabain exposure. Student's t-test, one tailed.

E) Alignments of Na⁺/K⁺ pump alpha subunits around the ouabain binding sites. Red indicates residues that are critical for higher sensitivity to ouabain, which are present in mouse Atp1a3 but not Atp1a1.

F) *In situ* hybridisation of *atp1a3a* at 24hpf (whole animal) and 5dpf brain (ventral view). Anterior is to the left. Scale bar = 0.5 mm (24 hpf); 0.1 mm (5 dpf). A-anterior; P-posterior; D-Dorsal; V-Ventral

G) CRISPR-Cas9 targeting of the *atp1a3a* resulted in a 19 bp deletion that eliminates the start codon (blue) and splice junction. Guide RNA target sequence and PAM sequence are shown as black bars. Sequence that is deleted in the mutant is indicated with a red bar.

H-I) Representative behavioural experiment showing *atp1a3a* ^{$\Delta 19/\Delta 19$} fish are hyperactive throughout the day-night cycle and have decreased sleep at night. Mean \pm SEM are shown.

J) *atp1a3a* ^{$\Delta 19/\Delta 19$} larvae sleep less at night due to shorter sleep bouts. Plotted are the genotype effect sizes (95% confidence interval) on each parameter relative to wild type. Shading indicates day (white) and night (grey). P-values are assigned by an F-test on the fixed effects coefficients from the linear mixed effects model. * $p<0.05$, ** $p<0.01$, *** $p<0.001$, ns $p>0.05$.

Dmist modulates Na⁺/K⁺ pump function and neuronal activity-induced sleep homeostasis

The similar night-time reduction in sleep in *dmist* and *atp1a3a* mutants, combined with the similarities between Dmist and Fxyd1, suggested that Dmist may regulate the Na⁺/K⁺ pump. We therefore exposed wild type and mutant larvae to pentylenetetrazol (PTZ), a GABA_A receptor antagonist that leads to globally heightened neuronal activity and elevated intracellular sodium levels that must be renormalized by Na⁺/K⁺ pump activity. Consistent with the hypothesis that Dmist and Atp1a3a subunits are important for a fully functional Na⁺/K⁺ pump, brains from both *dmist*^{i8/i8} and *atp1a3a*^{Δ19/Δ19} larvae had elevated intracellular sodium levels after exposure to PTZ (**Figure 6A**). Thus, neither *dmist* nor *atp1a3a* mutants were able to restore intracellular sodium balance after sustained neuronal activity as quickly as wild type siblings. Consistent with the night-specific alterations in sleep behaviour, we also found that baseline brain Na⁺ levels in *dmist* mutants were significantly elevated at night but not during the day (**Figure 6B**). Collectively, these data are consistent with the hypothesis that night-time sleep duration is affected by changes in Na⁺/K⁺ pump function and that Dmist is required to maintain this function both at night and after sustained high levels of neuronal activity.

We have previously shown in zebrafish that a brief exposure to hyperactivity-inducing drugs such as the epileptogenic PTZ or wake-promoting caffeine induces a dose-dependent increase in homeostatic rebound sleep following drug washout that is phenotypically and mechanistically similar to rebound sleep following physical sleep deprivation (Reichert et al., 2019). Based on their exaggerated intracellular Na⁺ levels following exposure to PTZ, we predicted that *dmist* mutants would also have increased rebound sleep in response to heightened neuronal activity. Upon wash-on/wash-off of lower dose (5 mM) PTZ, sleep rebound occurs in approximately 50% of wild type larvae (Reichert et al., 2019; **Figure 6C**, D). In contrast, all *dmist*^{i8/i8} larvae showed increased rebound sleep compared to *dmist*^{+/+} sibling controls (**Figure 6C-E**). Taken together with the elevated sodium retention experiments, such increases in rebound sleep induced by neuronal activity suggests that *dmist*^{i8/i8} fish more rapidly accumulate sleep pressure in response to heightened neuronal activity.

Finally, we predicted that if Dmist is affecting baseline sleep via modulation of Atp1a3a-containing Na⁺/K⁺ pumps, *dmist*^{-/-}; *atp1a3a*^{-/-} double mutants should have a reduction in night-time sleep that is not the sum of effects from either mutant alone. In other words, if Dmist and Atp1a3a are acting in separate pathways, the double mutant would have an additive phenotype, but if Dmist and Atp1a3a act together in the same complex/pathway, the mutant phenotypes should be non-additive. Indeed, *dmist*^{-/-}; *atp1a3a*^{-/-} mutants have a sleep reduction similar to that of *atp1a3a*^{-/-} mutants alone, consistent with a non-additive effect (**Figure 6F** and S6). Similar non-additivity can be also observed in the *dmist*^{-/-}; *atp1a3a*^{+/-} animals, which, like *atp1a3a*^{+/-} animals alone, have a milder sleep reduction, indicating that the lack of additivity between *dmist* and *atp1a3a* phenotypes is unlikely due to a floor effect, since double homozygous mutants can sleep even less (**Figure 6F**). This genetic interaction data is consistent with our hypothesis that Atp1a3a and Dmist act in the same pathway—the Na⁺/K⁺ pump—to influence sleep.

Discussion

Genetic screening discovers *dmist*, a novel sleep-regulatory gene

Using a reverse genetic viral screening strategy, we discovered a short-sleeping mutant, *dmist*, which has a disruption in a previously uncharacterized gene encoding a small transmembrane peptide. Given that the *dmist* mutant appeared within the limited number of 26 lines that we screened, it is likely that many other sleep genes are still waiting to be discovered in future screens. In zebrafish, one promising screening strategy will be to employ CRISPR/Cas9 genome

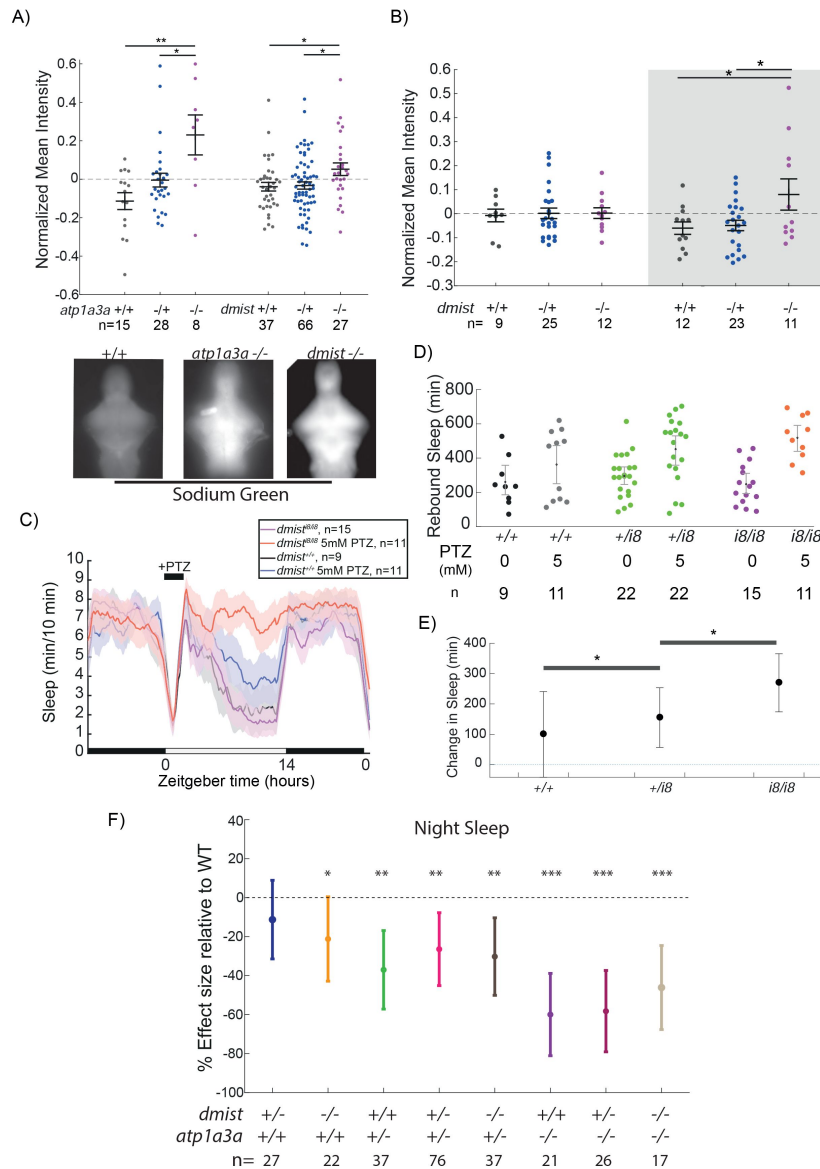


Figure 6.

***dmist* mutants have altered sodium homeostasis**

A) Brain sodium levels are significantly elevated after exposure to PTZ in both *atp1a3a*^{A19/Δ19} (2 independent experiments) and *dmist*^{i8/i8} (4 independent experiments) fish relative to wild type and heterozygous mutant siblings, as measured by fluorescence intensity of Sodium Green, normalized to the sample mean intensity. Crosses show mean ± SEM. n indicated the number of animals. Below are example images of brains stained with Sodium Green. *p<0.05, **p<0.01, one-way ANOVA, Tukey's post hoc test.

B) Under baseline conditions, brain sodium levels are significantly elevated in *dmist*^{i8/i8} fish at night but not during the day, as measured by fluorescence intensity with Sodium Green. Crosses show mean ± SEM. *p<0.05, **p<0.01, one-way ANOVA, Tukey's post hoc test.

C) *dmist*^{i8/i8} larvae have increased rebound sleep compared to wild type siblings following exposure to 5mM PTZ. Representative sleep traces of *dmist*^{+/+} (no drug, water vehicle controls in black; PTZ exposed in blue) and *dmist*^{i8/i8} (no drug in purple; PTZ exposed in red) following 1 hr exposure to 5 mM PTZ (black bar) in the morning. Data are mean ± SEM. *dmist*^{+/+} animals are not plotted for clarity but are included in panel D.

D) Rebound sleep after exposure to 5 mM PTZ, calculated from the experiment in C. Each dot represents a single fish, grey lines show mean ± SEM.

E) Effect size of change in sleep after 1 hr treatment with 5 mM PTZ (and washout) compared to vehicle treated controls (error bars show 95% confidence intervals). *p<0.05, one-way ANOVA, Tukey's post-hoc test.

F) Effect sizes (and 95% confidence interval) relative to wild types (dotted line) on sleep at night in larvae from *dmist*^{+/+}; *atp1a3a*^{+/+} in-crosses from 3 independent experiments. P-values are assigned by an F-test on the fixed effects coefficients from the linear mixed effects model relative to *dmist*^{+/+}; *atp1a3a*^{+/+} animals. For all sleep-wake parameters, see Figure S6. *p<0.05, **p<0.01, ***p<0.0001, ns p>0.05.

editing to systematically target candidate genes. Advances in the efficiency of this technology now makes it feasible to perform a CRISPR “F0 screen” in which the consequences of bi-allelic, gene-specific mutations are rapidly tested in the first generation, with only the most promising lines pursued in germline-transmitted mutant lines (Grunwald et al., 2019 [DOI](#); Jao et al., 2013 [DOI](#); Kroll et al., 2021; Shah et al., 2015 [DOI](#); Shankaran et al., 2017 [DOI](#); Wu et al., 2018 [DOI](#)). CRISPR F0 screens could be scaled to systematically target the large number of candidate sleep-regulatory genes identified through human GWAS studies and sequencing of human patients suffering from insomnia and neuropsychiatric disorders (Allebrandt et al., 2013 [DOI](#); Dashti et al., 2019 [DOI](#); Jansen et al., 2019 [DOI](#); Jones et al., 2019 [DOI](#); Lane et al., 2019 [DOI](#); Lek et al., 2016 [DOI](#); Palagini et al., 2019 [DOI](#)).

Dmist is related to the Na⁺/K⁺ pump regulator Fxyd1

The small Dmist transmembrane protein is highly conserved across vertebrates, expressed in neurons, and important for maintaining normal sleep levels. How can such a small, single pass transmembrane protein lacking any clear functional domains modulate the function of neurons and ultimately animal behaviour? The recognition that Dmist has sequence homology (~35% amino acid similarity; a conserved ‘RRR’ motif in the C-terminus) and structural homology (e.g. signal peptide and single pass transmembrane domains) to the Na⁺,K⁺-ATPase pump regulator Fxyd1 (Phospholemman) offers some important clues.

Fxyd1/Phospholemman is a member of the FXYP protein family, of which there are seven mammalian members (Sweadner and Rael, 2000 [DOI](#)). Each of the FXYP proteins is small, contains a characteristic FXYP domain, and has a single transmembrane domain. FXYP family members interact with alpha subunits of the Na⁺,K⁺ ATPase to regulate the function of this pump, with individual family members expressed in different tissues to modulate Na⁺,K⁺-ATPase activity depending on the physiological needs of the tissue (Geering et al., 2003 [DOI](#)). In cardiac muscle, FXYP1 is thought to act as a hub through which various signalling cascades, such as PKA, PKC, or nitric oxide, can activate or inhibit Na⁺ pump activity (Pavlovic et al., 2013 [DOI](#)). For example, FXYP1 is critical for mediating the increased Na⁺ pump activity observed after β -receptor stimulation via cAMP-PKA signalling (Despa et al., 2008 [DOI](#)). Much less is known about the role of FXYP1 in non-cardiac tissue, although it is expressed in neurons in the mammalian cerebellum, the choroid plexus, and ependymal cells, where it interacts with all three alpha subunits of the Na⁺,K⁺ ATPase (Feschenko et al., 2003 [DOI](#)).

In zebrafish, we also found that *fxyd1* is expressed in cells around the ventricles and in the choroid plexus (**Figure 4C** [DOI](#)), in contrast to *dmist* which is expressed in neurons throughout the brain. Despite the different expression patterns, mutation of each gene resulted in a similar reduction of sleep at night. However, unlike *dmist* mutants, which have fewer sleep bouts (i.e. initiate sleep less) and an increase in waking locomotor activity, *fxyd1* mutants have shorter sleep bouts (i.e. cannot maintain sleep) on average and do not have a locomotor activity phenotype. Just as the various FXYP family members modulate the Na⁺/K⁺ pump in different tissue- and context-specific ways, this phenotypic variation between *fxyd1* and *dmist* mutants could be due to the different *fxyd1* and *dmist* expression patterns, modulation kinetics of pump/channel dynamics, or interaction with different accessory proteins or signal transduction cascades. Nevertheless, the similar timing and magnitude of sleep reduction, combined with the structural similarity of Fxyd1 and Dmist, suggest that they may regulate similar sleep-related processes.

Dmist, the sodium pump, and sleep

The similarity between Dmist and FXYP1 led us to directly manipulate the Na⁺,K⁺ ATPase to test its importance in sleep. The Na⁺,K⁺-ATPase is the major regulator of intracellular Na⁺ in all cells and, by actively exchanging two imported K⁺ ions for three exported Na⁺ ions, is essential for determining cellular resting membrane potential (reviewed in Clausen et al., 2017 [DOI](#)). The Na⁺,K⁺-ATPase consists of a catalytic alpha subunit (4 known isoforms, ATP1A1-4), a supporting beta subunit (3 isoforms, ATP1B1-3), and a regulatory gamma subunit (the FXYP proteins). The alpha1

and alpha3 subunits are the predominant catalytic subunits in neurons (alpha2 is mostly restricted to glia), although the alpha1 subunit is also used ubiquitously in all tissues (McGrail et al., 1991 [\[1\]](#)). By mutating zebrafish orthologs of *Atp1a3*, we therefore could test the neuronal-specific role of the Na⁺,K⁺-ATPase in sleep.

Mutations in both zebrafish *Atp1a3* orthologs increased waking locomotor behaviour during the day. However, only mutations in *atp1a3a*, which is expressed brain-wide, but not in *atp1a3b*, which is expressed in more restricted brain regions, led to changes in night-time sleep. The *atp1a3a* mutants have a larger sleep reduction than *dmist*^{vir}, *dmist*ⁱ⁸, or *fyd1*^{A28} mutants, which is expected since loss of a pump subunit should have a larger effect than the loss of a modulatory subunit, as has been shown for other ion channels (Cirelli et al., 2005 [\[2\]](#); Wu et al., 2014 [\[3\]](#)). Autosomal dominant missense mutations leading to loss of function in *ATP1A3* cause movement disorders such as rapid-onset dystonia parkinsonism and childhood alternating hemiplegia (recurrent paralysis on one side) in humans (Canfield et al., 2002 [\[4\]](#); Heinzen et al., 2014 [\[5\]](#)), while loss of function mutations in *Atp1a3* result in generalised seizures and locomotor abnormalities, including hyperactivity, in mice, which was not observed in zebrafish (Clapcote et al., 2009 [\[6\]](#); Hunanyan et al., 2015 [\[7\]](#); Ikeda et al., 2013 [\[8\]](#); Kirshenbaum et al., 2011 [\[9\]](#); Sugimoto et al., 2014 [\[10\]](#)). A very high prevalence of insomnia was recently reported in patients with childhood alternating hemiplegia, some of which harboured mutations in *Atp1a3* (Kansagra et al., 2019 [\[11\]](#)), consistent with our observations that insomnia at night is a direct behavioural consequence of *atp1a3a* mutation in zebrafish. Since zebrafish *atp1a3a* mutants phenocopy the insomnia and hyperactivity phenotypes observed in patients, small molecule screens aimed at ameliorating zebrafish *atp1a3a* mutant phenotypes may be a promising approach for the rapid identification of new therapies for the management of this disease (Hoffman et al., 2016 [\[12\]](#); Rihel et al., 2010 [\[13\]](#)).

Together, the night-specific sleep phenotypes of *dmist*, *fyd1*, and *atp1a3a* mutants point to a role for the Na⁺,K⁺-ATPase in boosting sleep at night. How might the alpha3 catalytic subunit of the Na⁺/K⁺ pump regulate sleep, and how could *Dmist* be involved? We found that *Dmist* is required for proper maintenance of brain intracellular Na⁺ levels at night but not during the day, mirroring the timing of sleep disruption in *dmist*^{i8/i8} animals. This suggests that the decreased night-time sleep of *dmist* mutants is due to a specific requirement for *Dmist* modulation of the Na⁺/K⁺ pump at night. However, we cannot exclude the possibility that *Dmist*'s function is required in only a subset of critical sleep/wake regulatory neurons during the day that then influence behaviour at night, such as the wake-active, sleep-homeostatic regulating serotonergic neurons of the raphe (Oikonomou et al., 2019 [\[14\]](#)) or wake-promoting Hcrt/orexin neurons (Li et al., 2022 [\[15\]](#)). We also cannot exclude a role for *Dmist* and the Na⁺/K⁺ pump in developmental events that impact sleep, although our observation that ouabain treatment, which inhibits the pump acutely after early development is complete, also impacts sleep, argues against a developmental role. Another possibility is that disruption of proper establishment of the Na⁺ electrochemical gradient in *dmist* mutant neurons leads to dysfunction of various neurotransmitter reuptake transporters, including those for glycine, GABA, glutamate, serotonin, dopamine, and norepinephrine, which rely on energy from the Na⁺ gradient to function (Kristensen et al., 2011 [\[16\]](#)).

A third possibility is that *Dmist* and the Na⁺,K⁺-ATPase regulate sleep not by modulation of neuronal activity per se but rather via modulation of extracellular ion concentrations. Recent work has demonstrated that interstitial ions fluctuate across the sleep/wake cycle in mice. For example, extracellular K⁺ is high during wakefulness, and cerebrospinal fluid containing the ion concentrations found during wakefulness directly applied to the brain can locally shift neuronal activity into wake-like states (Ding et al., 2016 [\[17\]](#)). Given that the Na⁺,K⁺-ATPase actively exchanges Na⁺ ions for K⁺, the high intracellular Na⁺ levels we observe in *atp1a3a* and *dmist* mutants is likely accompanied by high extracellular K⁺. Although we can only speculate at this time, a model in which extracellular ions that accumulate during wakefulness and then directly signal onto sleep-

regulatory neurons could provide a direct link between Na^+, K^+ ATPase activity, neuronal firing, and sleep homeostasis. Such a model could also explain why disruption of *fyxd1* in non-neuronal cells also leads to a reduction in night-time sleep.

In addition to decreased night-time sleep, we also observed that *dmist* mutants have an exaggerated sleep rebound response following the high, widespread neuronal activity induced by the GABA-receptor antagonist, PTZ. Since both Atp1a3a and Dmist were essential for re-establishing proper brain intracellular Na^+ levels following PTZ exposure (**Figure 6A** [↗](#)), we speculate that the exaggerated sleep rebound is a consequence of increased neuronal depolarization due to defective Na^+ pump activity. This is consistent with our previous observations that the intensity of brain-wide neuronal activity impacts the magnitude of subsequent sleep rebound via engagement of the Galanin sleep-homeostatic output arm (Reichert et al., 2019 [↗](#)). Why does loss of *dmist* lead to both decreased night-time sleep and increased sleep rebound in response to exaggerated neuronal activity during the day? One possibility is that Na^+/K^+ pump complexes made up of different alpha and beta subunits may be differentially required for maintaining Na^+ homeostasis under physiological conditions and have different affinities for (or regulation by) Dmist. For example, the Atp1a1 subunit is considered the Na^+/K^+ pump workhorse in neurons, while Atp1a3, which has a lower affinity for Na^+ ions, plays an essential role in repolarizing neurons when Na^+ rapidly increases during high levels of neuronal activity, such as after a seizure (Azarias et al., 2013 [↗](#)). If Dmist preferentially interacts with Atp1a3a subunit, with which the non-additive effect of *dmist* and *atp1a3a* mutation on sleep is consistent, day-time sleep-related phenotypes in *dmist* mutants might be uncovered only during physiological challenge. Conversely, neurons may be more dependent on Atp1a3a and Dmist for sodium homeostasis at night due to changes in Na^+/K^+ pump composition, Dmist interactions, or ion binding affinities. For example, activity of the Na^+/K^+ pump can be modulated by the circadian clock (Damulewicz et al., 2013 [↗](#); Nakashima et al., 2018 [↗](#)), changes in substrate availability, including ATP (reviewed in Therien and Blostein, 2000 [↗](#)), or hormones (Ewart and Klip, 1995 [↗](#)). Teasing out how Dmist modulation of the Na^+/K^+ pump changes across the day-night cycle, and in which neurons Dmist's function may be particularly important at night, will require future investigation.

In conclusion, through a genetic screening strategy in zebrafish, we have identified a novel brain expressed gene that encodes a small transmembrane protein regulator of night-time sleep and wake behaviours. Future work will be required to uncover the precise signalling dynamics by which Dmist regulates the Na^+, K^+ -ATPase and sleep.

Acknowledgements

The initial screen, discovery, and characterization of *dreammist* was conducted in the lab of Alexander F Schier at Harvard University. We also would like to thank members of the Rihel lab and other UCL zebrafish groups for helpful comments on experiments and the manuscript.

We thank Shannon Shibata-Germanos for *fyxd1* mutant tracking experiments, John Parnavalas for reagents, Christine Orengo for help with small peptide sequence searches, Stuart Peirson for early access to mouse transcriptomic data, and Finn Mango Bamber for the Pokémon-card inspired *dreammist* name. The work was funded by NIH grants awarded to Alexander Schier (GM085357 and HL10952505); an ERC Starting Grant (#282027) and Wellcome Trust Investigator Award (#217150/Z/19/Z) to JR; NIH grant R35 NS122172 to DAP; and a Grand Challenges PhD studentship to ILB.

Zebrafish husbandry

All zebrafish lines were housed on a 14hr:10hr light:dark schedule in dechlorinated water at 27.5°C and routine husbandry was performed by the UCL Zebrafish Facility. Embryos were collected from spontaneous spawning and staged according to [Kimmel et al. 1995](#).

Embryos and larvae were raised on a 14hr:10hr light:dark schedule in 10cm Petri dishes at a density of 50 embryos per 10cm Petri dish. Embryo water (~pH7.3, temperature 28.5°C, conductivity ~423.7uS with methylene blue) was changed daily and animals over 4 days post fertilisation were euthanized by overdose of MS-222 (300 mg/l) or 15% 2-Phenoyethanol (77699 SIGMA-ALDRICH) at the end of experiments.

Raising of genetically altered zebrafish and all experimental procedures were performed under project licence 70/7612 and PA8D4D0E5 awarded to JR under the UK Animals (Scientific Procedures) Act 1986 guidelines.

Lines

The *dmist^{vir}* allele was generated in wild type line T/AB-5 ([Varshney et al., 2013](#)) and outcrossed to Harvard AB. The *dmistⁱ⁸*, *fxyd1^{Δ28}*, *atp1a3a^{Δ19}*, and *atp1a3b^{Δ14}* alleles were generated and maintained at UCL on an AB/TL background. Both *dmistⁱ⁸* and *dmist^{vir}* were out-crossed to the AB strain at UCL for at least 3 generations.

Larval Zebrafish Behavioural Tracking

At 4 days post fertilisation (dpf), zebrafish larvae were placed into individual wells of a 96-square well plate (WHA7701-1651 Sigma-Aldrich) filled with 650 µl of embryo water per well and tracked for 3 days under a 14:10 light:dark schedule (lights on-09:00, lights off-23:00) using automated videotracking in ViewPoint ZebraBoxes (Viewpoint Life Sciences). The 96-well plate was under constant illumination with infrared LEDs, and white LEDs simulated the light:dark schedule. Videography (with one-third inch Dragonfly2 PointGrey monochrome camera, frame rate: 25-30 Hz; fixed-angle megapixel lens, Computar M5018-MP) of individual behavior was recorded in quantization mode to detect movement by background subtraction between frames in individual wells with 60 second integration time bins. Parameters used for detection were calibrated according to the sensitivity of individual boxes but were in the following range: detection threshold, 15-20; burst, 50 pixels; freeze, 3-4 pixels. Embryo water in the wells was topped up daily with fresh water, and ambient room temperature was maintained at approximately 26°C. Output data was sorted, parsed and analysed by custom Perl and Matlab scripts (MATLAB R2016 version 9.1, The MathWorks), as in [Rihel et al. 2010](#).

Oxygen-permeable lids (Applied Biosystems 4311971) were applied over the top of the 96-well plate when performing experiments in constant darkness, and the larvae were left undisturbed for the duration of the experiment to avoid light exposure.

At the end of the experiment, all larvae were visually checked for health before euthanasia and transfer to individual wells of a 96-well PCR plate for DNA extraction and genotyping.

Behavioural analysis


Sleep parameters were calculated as in [Rihel et al. 2010](#). For each genotype, exemplar experiments are shown, and summary data was analysed by combining experiments with a linear mixed effects model as follows. Behavioural summaries across multiple experiments were determined by using the Matlab fitlme function to fit a linear mixed effects model for each

parameter with genotype as a fixed effect and independent experiment as a random effect, then representing the effect size as a % change from the wild type value. Before fitting the linear mixed effects model, the parameters sleep, sleep length, and waking activity were log normalized by calculating the log of 1+ the parameter value for each larva.


Circadian period for every larva was calculated using the Matlab findpeaks function on the activity (delta-pixels) timeseries data with a minimum peak distance of 18 hours (1080 minutes). N-way ANOVA was calculated to evaluate differences between groups.


Code and data are available at <https://github.com/ilbarlow/Dmist> .

Adult behavioural tracking

Fish from a *dmist*^{i8/+} x *dmist*^{i8/+} cross were raised in a mixed gender tank to adulthood. Zebrafish adults (aged 3-4 months) were randomly selected and tracked on a 14:10 light:dark cycle (180 lux at water surface, lit from above) for three days as in (Chiu et al., 2016 ) . In brief, fish were placed into uncovered plastic chambers (7x12x8.5 cm; WxLxH) with small holes for water exchange, and these were placed in a circulating water tank (46x54 cm with 4.5 cm water height). This setup was supplied with fish water from the home aquarium heated to 28°C and pumped from a 45 L reservoir at a flow rate of 1.3 L/min. Infrared light (60 degree, 54 LED Video Camera Red Infrared Illuminator Lamp, SourcingMap, with the ambient light detector covered) was continuously supplied from below. Fish were tracked at 15 Hz using Viewpoint Life Sciences ZebraBox tracking software in tracking mode, with a background threshold of 40, inactive cut-off of 1.3 cm/sec, and a small movement cut-off of 8 cm/sec. Each track was visually inspected for errors at one-minute resolution across the entire session and analysed using custom Matlab scripts (MATLAB R2016 version 9.1, The Mathworks, Inc). Experiments were performed blind to genotype, which was determined by fin-clip after the experiment. Females and males were originally analysed separately; since no significant gender effect was found (two-way ANOVA, genotypeXgender), data from both genders were pooled for the final analysis.

Genotyping

Prior to genotyping, adult fish were anaesthetised in 30 µg/ml MS-222, fin-clipped by cutting a small section of the caudal fin, and then allowed to recover in fresh fish water. For pooled experiments, 3 dpf larvae from heterozygous in-crosses were fin-clipped as in Wilkinson et al., 2013 ) and allowed to recover in a square 96-well plate to keep larvae separate prior to pooling larvae of the same genotype. Genomic DNA was extracted from adult fin clips and larvae by boiling for 30 minutes in 50 µl 1X base solution (0.025 M KOH, 0.2 mM EDTA). Once cooled, an equal volume (50 µl) of neutralisation buffer (0.04 M Tris-HCl) was then added and undiluted genomic DNA used for genotyping.

The *dmist*^{vir} genotype was detected by PCR (standard conditions) using a cocktail of three primers (0.36 mM final concentration each primer) to detect the wild type allele and viral insertion (see **Table 2** ) so that genotypes could be assigned according to size of bands detected (*dmist*^{vir/vir} 800 bp; *dmist*^{vir/+} 508 bp and 800bp; *dmist*^{+/+} 508 bp).

The *dmist*ⁱ⁸ genotype was assigned by KASP genotyping using allele-specific primers (*dmist*ⁱ⁸ allele 5'-GATCTCCCT[GCAGAAAGAT]CTTCTGCA-3' = FAM, *dmist*⁺ allele 5'-GATCTCCCT[CACCG]CTTCTGCA-3' = HEX; KASP master mix KBS-1016-011) and assay were prepared and analysed according to manufacturer's protocol (LGC genomics).

The *atp1a3a*^{Δ19} genotype was assigned by KASP genotyping using allele-specific primers (*atp1a3a*^{Δ19} allele 5'-GACAGACTGAAGAAACAGCGACTGACGGCTC[CAAAATGGGGGTAAGAGTC]-3' = FAM, *atp1a3a*⁺ allele 5'-GACAGACTGAAGAAACAGCGACTGACGGCTC-3'[] = HEX).

Strain designation	Allele Number	Gene identifier	Additional Information
<i>10543/dmist^{vir}</i>	<i>la015577Tg</i>	ENSDARG00000095754	Maintained at UCL
<i>dmistⁱ⁸</i>	<i>u505</i>	ENSDARG00000095754	Maintained at UCL
<i>fxyd1^{Δ28}</i>	<i>u504</i>	ENSDARG00000099014	Maintained at UCL
<i>atp1a3a^{Δ19}</i>	<i>u513</i>	ENSDARG00000018259	Maintained at UCL
<i>atp1a3b^{Δ14}</i>	<i>u514</i>	ENSDARG00000104139	Maintained at UCL

Table 1.

Zebrafish lines

	Oligo Name	Sequence (5' -> 3')	Annealing temperature (°C)	Application
1	dmist_vir_fw	CACAGGGATGTGATGCCGGTTAAC	55	dmistvir genotyping
2	dmist_vir_rev	GTAGACACATACTGCCATACCAATC	55	dmistvir genotyping
3	vir_fw	CACCAGCTGAAGCCTATAGAGTACGAGC-	55	dmistvir genotyping
4	dmist_Dr_5RACE_fw	CGTTTCGCCACAATGTCAGCA	55-65	dmist_Dr 5'RACE
5	dmist_Dr_5RACE_rev_outer	AATGTTCAACTCCAGGCGTC	55-65	dmist_Dr 5'RACE
6	dmist_Dr_5RACE_rev_inner	AATGTTCAACTCCAGGCGTC	55-65	dmist_Dr 5'RACE
7	dmist_Dr_3RACE_fw_inner	GACGCCTGGAGTTGAACATT	55-65	dmist_Dr 3'RACE
8	dmist_Dr_3RACE_fw_outer	GGTATGGCAGTATGTGTCTACA	55-65	dmist_Dr 3'RACE
9	Dmist_Mm_3RACE_outer	GCTGGTGACTGTCTCTTATG	55-65	dmist_Mm 3'RACE
10	Dmist_Mm_3RACE_inner	GTGTCTACAAGCCCATCCGTC	55-65	dmist_Mm 3'RACE
11	dmist_Dr_fw	TTTCGCCACAATGTCAGCAGC	56	dmist_Dr probe
12	dmist_Dr_rev	CGACTTTCATTTATTAGTTCAGACATGTC	56	dmist_Dr probe
13	qPCR_dmist_fw	ACGCCAGACCTTATGAAATCC	60	RT-qPCR
14	qPCR_dmist_rev	TGCGTCGGAGAGGTTTGTAG	60	RT-qPCR
15	qPCR_ankrd13a_fw	TGGTGGCGTTCCAGAGTTAC	60	RT-qPCR
16	qPCR_ankrd13a_rev	GGACACGAGAGGAATCCAGC	60	RT-qPCR
17	qPCR_slc6a4b_fw	ACATGGTTGGGTCGACGTTT	60	RT-qPCR
18	qPCR_slc6a4b_rev	TCCAACCCACCAAAAGTGCT	60	RT-qPCR
19	ef1alpha_fw	TGCTGTGCGTGACATGAGGCAG	60	RT-qPCR
20	ef1alpha_rev	CCGCAACCTTTGGAACGGTGT	60	RT-qPCR
21	SP6dmist_sgRNA	ATTTAGGTGACACTATAGCGTTATGCAGAAAGCGGTGGTTTTAGAGCTAGAAATAGCAAG	n/a	CRISPR
22	T7atp1a3a_sgRNA	TAATACGACTCACTATAGACTGACGGCTCCAAAATGGGTTTTAGAGCTAGAAATAGCAAG	n/a	CRISPR
23	SP6fyd1_sgRNA	ATTTAGGTGACACTATAGGACCCTCTGCCAACACAAGGTTTTAGAGCTAGAAATAGCAAG	n/a	CRISPR
24	SP6atp1a3b_sgRNA	ATTTAGGTGACACTATAGGACTGACTGCCAACCATGGTTTTAGAGCTAGAAATAGCAAG	n/a	CRISPR
25	HRM_dmist_fw	GCCACAATGTCAGCAGCACG	59	HRM
26	HRM_dmist_rev	GCGTTCACCTTTAGACTCTCCCAGC	59	HRM
27	HRM_atp1a3a_fw	TGACAGACTGAAGAAACAGC	55	HRM
28	HRM_atp1a3a_rev	TTAAATCTCAGCACCCAGCAG5	55	HRM
29	HRM_fxyd1_fw	TGACCAAACCTTCTTAAGGTGC	58	HRM
30	HRM_fxyd1_rev	AAATTGAGAAGACTTACTGGTCTGC	58	HRM
31	HRM_atp1a3b_fw	AAAGGCTGTCACCTTCTCCATCAC5	58	HRM
32	HRM_atp1a3b_rev	TGCAGTAGATGAGGAATCGGTC	58	HRM
33	MiSeq_dmist_fw	TCGTCGGCAGCGTCAGATGTGTATAAGAGACAGTAACTTACGTGTGGACGGACTC	58	MiSeq
34	MiSeq_dmist_rev	GTCTCGTGGGCTCGGAGATGTGTATAAGAGACAGTTGCCTCAGCAGGATTTTCATAAG	58	MiSeq
35	MiSeq_atp1a3a_fw	TCGTCGGCAGCGTCAGATGTGTATAAGAGACAGTCGTTATCCGTGCAAGAGCTTC	58	MiSeq
36	MiSeq_atp1a3a_rev	GTCTCGTGGGCTCGGAGATGTGTATAAGAGACAGTTCTCAGCACCAGCAGTTATCG	58	MiSeq
37	MiSeq_atp1a3b_fw	TCGTCGGCAGCGTCAGATGTGTATAAGAGACAGTACTGACATTCTCTTTCGTG	68	MiSeq
38	MiSeq_atp1a3b_rev	GTCTCGTGGGCTCGGAGATGTGTATAAGAGACAGTTCTCTGTATGCAGTAGATGAGG	68	MiSeq
39	MiSeq_fxyd1_fw	TCGTCGGCAGCGTCAGATGTGTATAAGAGACAGAAATACTGTCTTGTGACCAAACC	57	MiSeq
40	MiSeq_fxyd1_rev	GTCTCGTGGGCTCGGAGATGTGTATAAGAGACAGTTATCTCTGCTGCAAAATGC	57	MiSeq
41	attB1-dreammist forward primer	GGGGACAAGTTTGTACAAAAAAGCAGGCTTCACCATGTCAGCAGCAGCGCTGATCTCC	55-60	Gateway
42	attB3-dreammist reverse primer	GGGGACCACTTTGTACAAGAAAGCTGGGTATCACCTGCGTCGGAGAGGTTTGTAG	55-60	Gateway
43	Dmist-GFPA22Wfw	GCTTTTCCAGTCTGGGAGTTGGCAGCTGGGAGAGCTAAAG	66	SDM
44	Dmist-GFPA22WRev	CTTTAGACTCTCCAGCTGCCAACTCCAGACTGGAAGG	66	SDM

Table 2.

Primer Sequences

The *atp1a3b*^{Δ14} genotype was assigned by PCR using MiSeq_atp1a3b primers (Table 2) , with the *atp1a3b*^{Δ14} allele running 14 bp faster than the *atp1a3b*⁺ allele.

fxyd1^{Δ28} was assigned by KASP genotyping using allele-specific primers (*fxyd1*^{Δ28} allele 5'-GAAGGTCGGAGTCAACGGATTAAATAAACTTTATTGTGCTTTTGTAGTTGT[A]-3' = HEX, *fxyd1*⁺ allele 5'-GAAGGTGACCAAGTTCATGCTTAATAAACTTTATTGTGCTTTTGTAGTTGT[G]-3' = FAM) or PCR using MiSeq_fxyd1 primers (see Table 2) followed by digestion with the restriction enzyme DrdI, which yields bands at 138 bp and 133 bp for *fxyd1*^{+/+}; 138 bp, 133 bp and 271 bp for *fxyd1*^{+/Δ28}, and 243 bp for *fxyd1*^{Δ28}.

3 race

FirstChoice RLM-RACE kit (Ambion AM1700) was used to amplify the 5' and 3' ends from cDNA obtained from 4 dpf larvae raised on a 14:10 LD cycle and C57BL/6 E13.5 mouse embryos obtained from the Parnavalas lab (UCL). 5' and 3' RACE primers were designed according the manufacturer's guidelines (Table 2) and the manufacturer's protocol was followed. Clones were sequenced by Sanger sequencing.

In situ hybridisation

Probes were designed to target the 3'UTR and entire open reading frame (ORF) of *dmist*_Dr transcript using primers that amplified the target region from zebrafish cDNA under standard PCR conditions (expected size 1325 bp; Table 2) . The PCR product was cloned into pSC vector (Strataclone PCR cloning kit Agilent 240205-12) and verified by Sanger sequencing. Antisense probe was generated by cleavage of pSC-dmist plasmid with XbaI and *in vitro* transcribed with T3 polymerase (Promega P2083) using 1 µg DNA template according to the standard *in vitro* transcription protocol (see the full protocol at [dx.doi.org/10.17504/protocols.io.ba4pigvn](https://doi.org/10.17504/protocols.io.ba4pigvn)). RNA probe was extracted and purified using the ZYMO RNA concentrator kit (Zymo #R1013).

Whole mount *in situ* hybridisation was performed according to (Thisse and Thisse, 2008) with the following adaptations. Embryos less than 5 dpf were dechorionated and fixed at the appropriate stage in 4% paraformaldehyde (PFA) overnight at 4°C. 5 dpf larvae were fixed in 4% PFA/4% sucrose overnight at 4°C and then washed 3x5 min in PBS prior to dissecting out the brain. Fixed embryos were washed 3x5 min in PBS, progressively dehydrated into 100% methanol (MeOH) and stored at -20°C overnight. Prior to pre-hybridisation embryos were bleached for 30 min in the dark (0.05% formamide, 0.5X SSC, 6% H₂O₂) and then fixed in 4% PFA for 30 min at room temperature. To image, the embryos were progressively rehydrated into 0.1% PBTw, progressively sunk in to 80% glycerol, and imaged on a Nikon compound microscope (Nikon Eclipse Ni, Leica MC190HD camera).

RT-qPCR

Larvae from heterozygous in-crosses (*dmist*^{i8/+} or *dmist*^{vir/+}) were genotyped by tail biopsy at 3 dpf (Wilkinson et al., 2013) and allowed to recover fully in individual wells of a square wellled 96-well plate before euthanizing at 5 dpf. RNA was extracted from three 5 dpf embryos of each genotype by snap freezing in liquid nitrogen and TRIzol RNA extraction (Ambion 15596026) with the following modifications to the manufacturer's protocol: 400 µl total TRIzol reagent used to homogenise larvae using a pellet pestle homogenizer, and 5 µg glycogen (Invitrogen Cat No. 10814010; 20 µg/µl) was added to the RNA solution after chloroform extraction to aid precipitation of the RNA. The cDNA library was synthesised from high quality RNA (Agilent AffinityScript qPCR cDNA synthesis kit 600559), diluted 1:10, and gene-specific primers (Table 2) were used for amplification of target genes with SYBR green mastermix in a BioRad CFX Real-Time qPCR instrument. Gene expression levels were normalised to the housekeeping gene *ef1alpha* (primers in Table 2) and analysed using custom Matlab scripts (MATLAB v9.2 2017, The Mathworks 2017).

Sodium Green Assay

Cell permanent Sodium Green tetraacetate (Invitrogen, S6901) was prepared fresh from frozen stock by dissolving in DMSO to 1 mM then diluting in fish water to a final concentration of 10 μ M. About 50 larvae (5–7 dpf) from *atp1a3a* ^{Δ 19/+} or *dmist*^{*i8/+*} in-crosses were placed in wells of a 6 well plate, then most fish water was removed and replaced with 3 mL of the 10 μ M Sodium Green solution for two hours. During exposure, the plate was covered in foil and placed in a 28°C incubator. For PTZ experiments, larvae were also exposed to 10 mM PTZ (diluted from 1 mM stock dissolved in water) for two hours. For timepoints at night (ZT17–19), larvae were handled and collected under red light. After soaking in Sodium Green, larvae were washed 3X with fish water, anaesthetised with MS-222, and fixed in 4% PFA/4% sucrose overnight at 4°C. After 3X wash in PBS, larval brains were dissected and placed in 200 μ L PBS in a 48 well plate, and the matched bodies were used for genotyping (see *Genotyping*). Brains were imaged using an upright MVX10 MacroView microscope with an MC PLAPO 1x objective (both OLYMPUS) with a mercury lamp for fluorescent excitation at 488 nm (OLYMPUS, U-HGLGPS). Images of roughly the same focal plane (dorsal/ventral view) were taken with an XM10 OLYMPUS camera by a single exposure following minimal light exposure (to avoid bleaching). Mean fluorescent intensity was calculated from ROIs placed on the optic tectum/midbrain using ImageJ, background subtracted and normalized to the average fluorescence intensity for each imaging session.

Protein Alignments

Cross-species *dmist* homologues were identified by reciprocal BLASTp of the C-terminal region of *Dmst_Dr* in vertebrate genomes. Translations of candidate transcript open reading frames were then aligned with *Dmst_Dr* using ClustalOmega to calculate the percentage identity matrix (www.ebi.ac.uk/Tools/msa/clustalo/) (<http://www.ebi.ac.uk/Tools/msa/clustalo/>) and visualised with the tool Multiple Align Show (www.bioinformatics.org/sms/multi_align.html) (http://www.bioinformatics.org/sms/multi_align.html).

To identify *Dmst* orthologues, *Dmst* peptides were aligned with the multiple sequence alignment tool MAFFT (Katoh and Toh, 2010) and seeded into a JackHMMR iterative search of the Uniprot database (Johnson et al., 2010). Protein-protein alignments of *Dmst* to *Fxyd1* were then performed using ClustalOmega and visualized with the tool Multiple Align Show.

CRISPR/Cas9 gene targeting

CRISPR targets were designed and synthesised according to Gagnon et al., 2014 using ChopChop (Montague et al. 2014; <http://chopchop.cbu.uib.no/>; see **Table 2** for sequences) to identify target sites. 100 pg sgRNA and 300 pg Cas9 mRNA (pT3TS-nCas9n) were injected into the yolk of 1-cell stage AB-TL embryos obtained from natural spawning. F0 fish were screened by high resolution melt (HRM) analysis using gene-specific primers (**Table 2**) with Precision melt supermix (Biorad 1725112) according to the manufacturer's protocol in a BioRad CFX RT-PCR thermocycler. Positive founders identified in HRM analysis were then sequenced by Illumina MiSeq using gene specific primers with adapters (**Table 2**) according to the manufacturer's protocol.

Molecular cloning

GFP was fused to the *Dmst_Dr* open reading frame (ORF) by Gateway cloning (Kwan et al., 2007). Gene-specific primers were designed to amplify a PCR product that was recombined with middle donor vector (**Table 2**; Invitrogen Gateway pDONR221 Cat No. 12536017, Invitrogen Gateway BP Clonase II Cat No. 11789020) to generate a middle entry clone (pME-*Dmst*). pME-*Dmst* was recombined with 5' (p5E-CMV/SP6) and 3' (p3E-GFPpA) entry clones and destination vector (pDestTol2pA2) using Gateway Technology (Invitrogen LR Clonase II Plus enzyme Cat No. 12538200) following the manufacturer's protocol.

A 3 bp mutation was introduced into the *CMV:dreammist-GFPpA* by inverse PCR using specific primers (Table 2) and KOD high fidelity hot start polymerase (Millipore 71085). The template was degraded by DpnI digest and circular PCR product was transformed into OneShot TOP10 chemically competent E coli (Invitrogen C4040). Both *CMV:dreammist-GFPpA* and *CMV:dreammistA22W-GFPpA* constructs were checked by Sanger sequencing.

For labelling the plasma membrane, mRNA was *in vitro* transcribed from pCS2-myr-Cherry linearised with NotI, *in vitro* transcribed with SP6 mMessage mMachine (Ambion AM1340), purified and quantified with a QuBit spectrophotometer, and injected at 0.04 µg/µL.

Microinjection and imaging

For Dmist-GFP and DmistA22W-GFP live imaging, embryos from an AB-TL in-cross were injected with 1 nL of plasmid (7 ng/µL). After developing to 90% epiboly, the embryos were placed on a glass coverslip and observed on an inverted confocal microscope (SPinv, Leica) with a 40X objective.

RNAseq

Larvae from heterozygous in-crosses (*dmist^{i8/+}* x *dmist^{i8/+}* and *dmist^{vir/+}* x *dmist^{vir/+}*) were raised to adulthood, genotyped and then homozygous mutant and wild type siblings were kept separate. Homozygous mutant and wild-type sibling fish were then in-crossed so that first cousins were directly compared. RNA was extracted from thirty 6 dpf larvae using the same protocol as for RT-qPCR and sent for RNAseq analysis at the UCL Institute of Child Health with a sequencing depth of 75 million reads per sample. Differential analysis of transcript count level between groups was performed as in (Love et al., 2014), and additional analysis was performed using custom Matlab scripts (MATLAB v9.2 2017, The Mathworks 2017).

Mouse RNAseq analysis

The dataset was downloaded from https://web.stanford.edu/group/barres_lab/brain_rnaseq.html; (Zhang et al., 2014) and hierarchical clustering (average linkage) and Pearson correlation calculation analysis were performed using custom Matlab scripts (MATLAB v9.2 2017, The Mathworks 2017).

Experimental Design and Statistical Analyses

Data was tested for normality using the Kolmogorov-Smirnov test. If data were normally distributed, N-way ANOVA (alpha=0.05) was used with correction for multiple comparisons using Tukey's test. If non-parametric, the Kruskal-Wallis test was used with correction for multiple comparisons using Dunn-Sidak (alpha=0.05). Outliers were removed by Grubb's test (threshold $p < 0.01$). P values from the linear mixed effects models were determined by an F-test on the fixed effects coefficients generated from the linear mixed effects model in Matlab.

Data were grouped by genotype and gender for adult experiments and grouped by genotype and day of experiment for larval experiments.

All code is available at <https://github.com/ilbarlow/Dmist>.

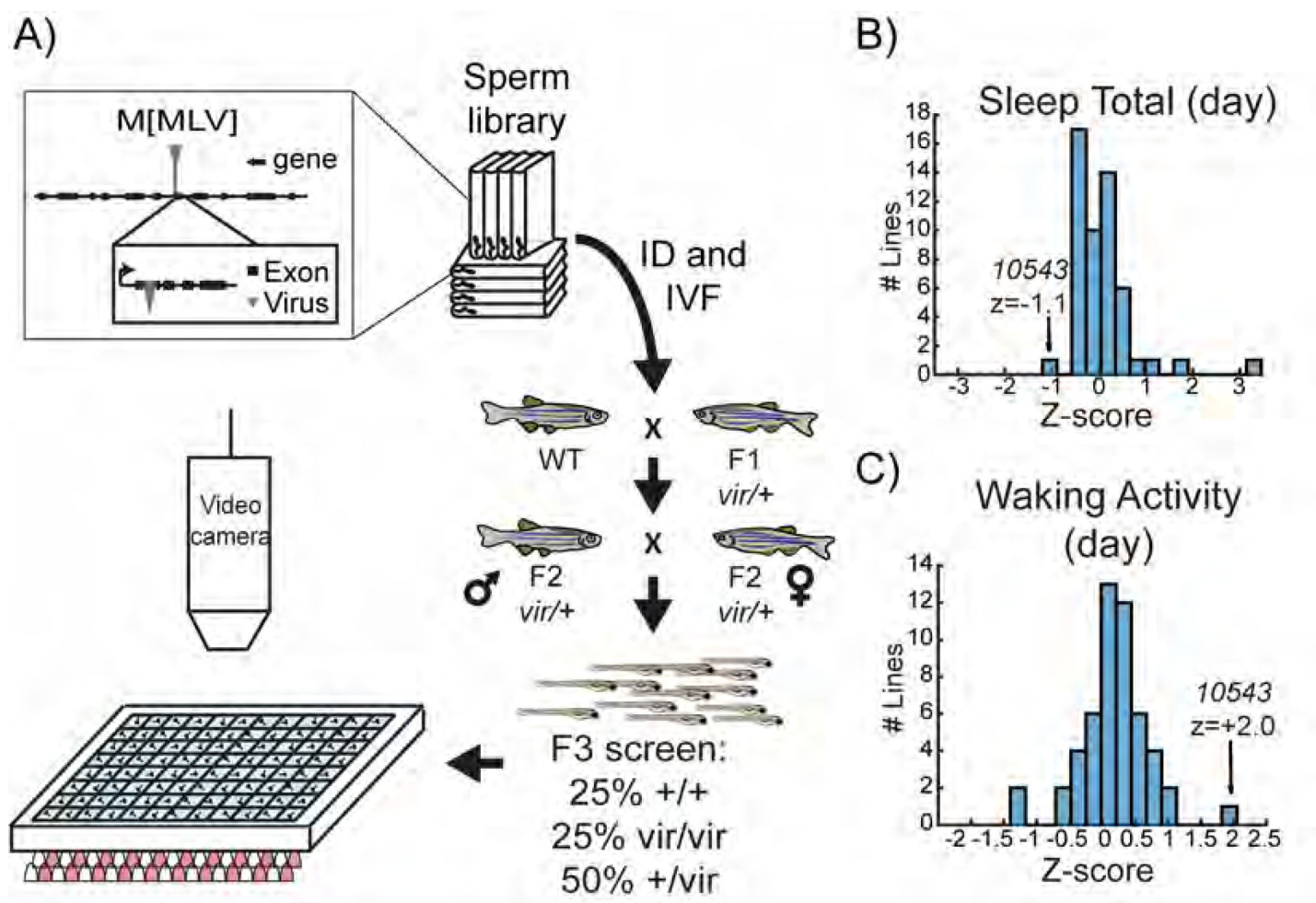


Figure S1.

A viral insertion screen for sleep-wake regulators

A) Schematic of screening strategy. Candidate genes were selected from a list of 904 mammalian genes encoding protein classes most often linked to behavioural regulation, including 1) genes previously implicated in sleep and circadian rhythms; 2) G-protein coupled receptors; 3) neuropeptide ligands; 4) channels; and 5) proteins involved in post-translational regulation, such as de-ubiquitinating enzymes (Supplemental Data 1). tBLASTN of the human protein sequences identified 1162 zebrafish orthologs (Zv6), of which 702 (60.4%) had viral insertions mapped in the 'Zenemark' zebrafish viral insertion library (Varshney et al., 2013). Sperm harbouring viral insertions in 26 loci were successfully used for *in vitro* fertilization and propagated to the F3 generation for screening. F3 larvae from single family F2 in-crosses were monitored on a 14hr:10hr light:dark cycle from 4-7 dpf using videography and genotyped at the end of the experiment.

B-C) Histogram of total daytime sleep (B) and average daytime waking activity (C) normalized as standard deviations from the mean (Z-score) of all the viral-insertion lines tested (including heterozygous *vir/+* and homozygous *vir/vir*). Line 10543 (renamed *dreammist*) exhibited decreased daytime sleep and increased daytime waking activity.

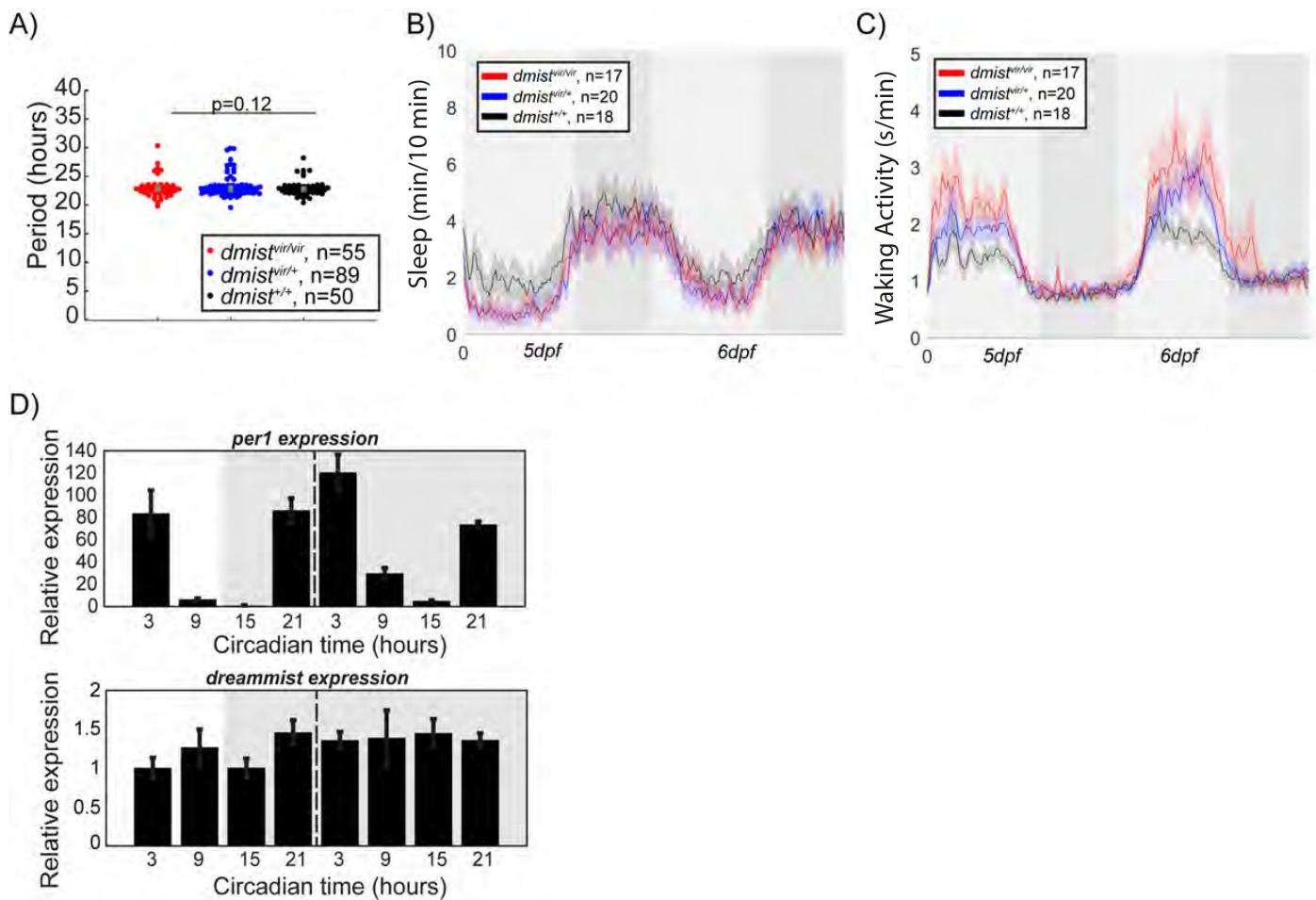


Figure S2.

dmist^{vir/vir} fish are hyperactive and have normal circadian rhythms.

A) Free-running circadian period length of the locomotor activity of larvae from a *dmist^{vir/+}* in- cross following the transition at 5 dpf from a 14hr:10hr light:dark cycle to constant dark conditions. The data is quantified for 48 hours after the shift to darkness and shows no difference in period between *dmist^{vir/vir}* larvae and their sibling controls. Data is from 3 independent experiments. $p > 0.05$, one-way ANOVA, Tukey's post hoc test.

B-C) Representative mean \pm SEM sleep (B) and waking activity (C) traces of animals used to calculate circadian period length in (A). Light and dark grey blocks show subjective day and night, respectively.

D) RT-qPCR time-course before (light) and after (grey) transfer into constant dark demonstrates that *dmist* mRNA levels do not oscillate with a circadian period, unlike *per1* mRNA which does. $n = 3$ replicates per timepoint. Expression is normalized to circadian time 3. Data are mean \pm SEM.

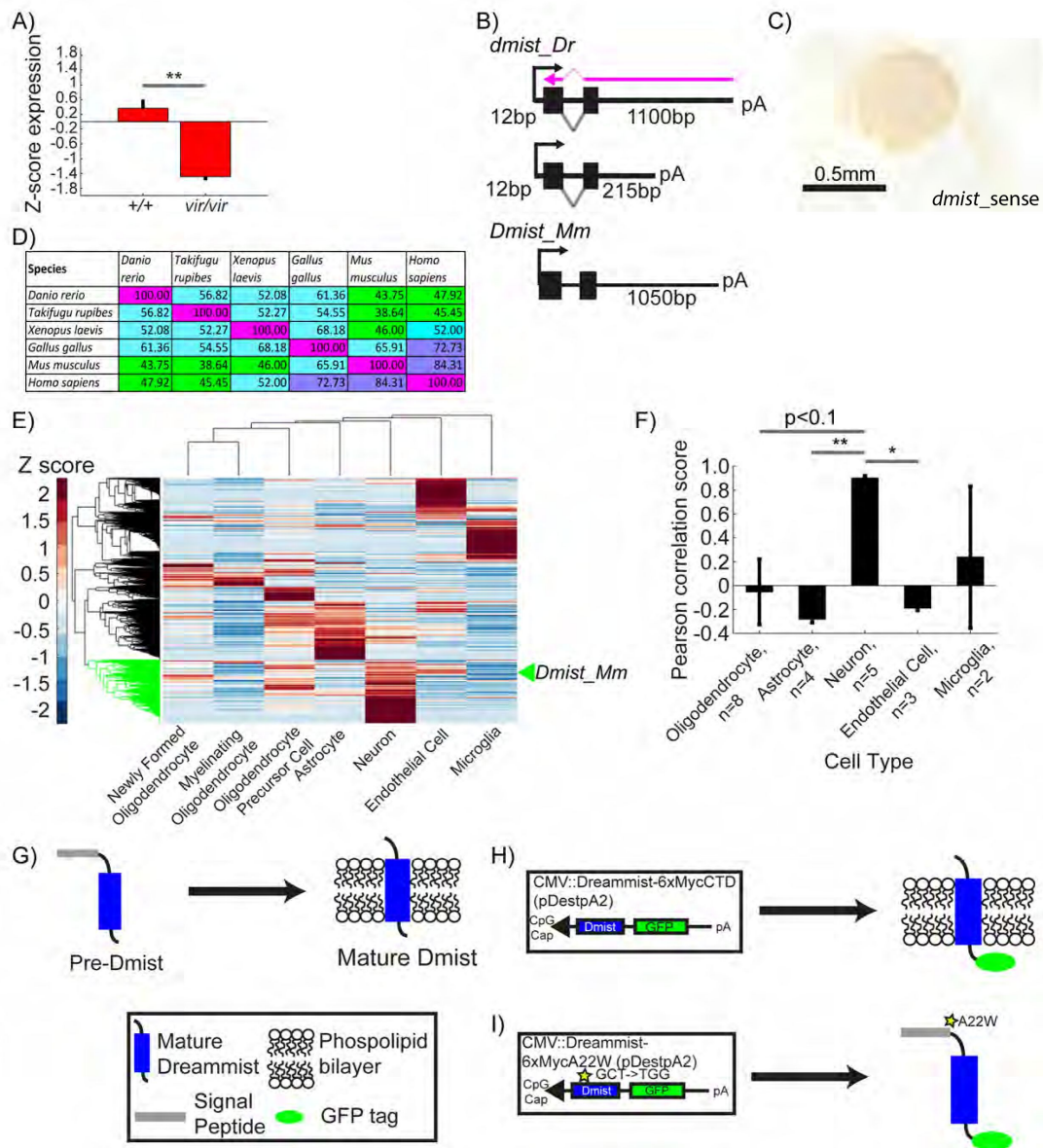


Figure S3.

dmist is enriched in neurons and requires the signal peptide cleavage site for membrane localisation.

A) Relative expression level of *dmist* transcript from RNA sequencing of 6 dpf *dmist*^{vir/vir} and *dmist*^{+/+} siblings. Z-scores were calculated by subtracting mean expression and normalising by the standard deviation across all expressed transcripts (27,243 transcripts). Data show mean \pm SEM from 3 independent biological replicates. ** $p < 0.01$ Student's t-test.

B) 3' and 5' RACE identify a long (1100 bp) and short (215 bp) 3'UTR variant in *dmist_Dr*, and a long 3'UTR (1050 bp) in *Dmist_Mm*. The purple arrow indicates the ISH probe used in Figure 2D.

C) *dmist_Dr* sense probe negative control at 24 hpf shows no detectable expression.

D) Percentage identity matrix comparing *Dmist* homologues across 6 vertebrate species (100%=magenta; >70%=purple; >50%=cyan; <50%=green).
 E) Hierarchical clustering of RNAseq dataset of 6 different cell types isolated from the developing (E13.5) mouse brain (Zhang et al., 2014) and post-hoc identification of *Dmist_Mm*. Data was standardized by subtracting the mean expression and normalizing by the standard deviation across all expressed transcripts in each cell type (column). *Dmist_Mm* (green arrow) co-clusters with genes highly expressed in neurons (green shaded branches).
 F) Pearson rank correlation of canonical cell-type markers with *Dmist_Mm* shows high co-expression with neuronal markers compared to astroglial and endothelial cell markers. Data are mean \pm SEM. * $p < 0.05$, ** $p < 0.01$; Kruskal-Wallis, Dunn-Sidak post-hoc test.

G-I) Predicted processing of Dmist to its mature form in the plasma membrane (G). C-terminal GFP fusion to Dmist is predicted to localise to the membrane (H). However, a mutation (A22W) at the signal peptide cleavage site (I) is predicted to inhibit signal peptide cleavage and so prevent proper subcellular localisation of the mature protein.

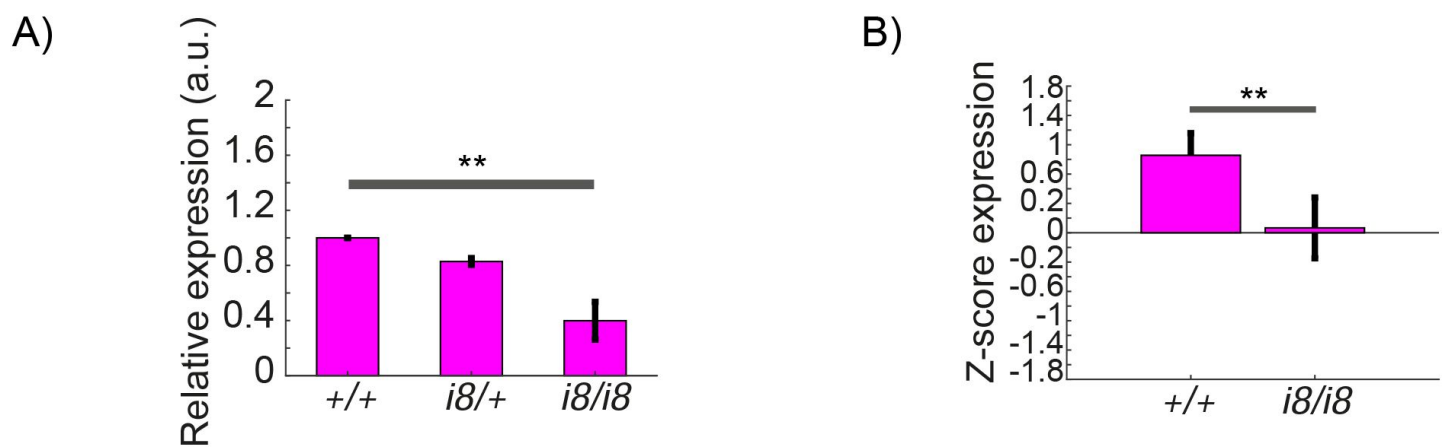


Figure S4.

CRISPR-generated *dmist* mutants have reduced *dmist* transcript levels

A) RT-qPCR shows *dmist*^{i8/i8} larvae have reduced *dmist* mRNA levels, suggesting that *dmist*ⁱ⁸ transcripts undergo nonsense mediated decay. Data are mean \pm SEM of three biological replicates. ** $p < 0.01$; one-way ANOVA, Tukey's post-hoc test.

B) Relative expression level of *dmist* transcript from RNA sequencing of 6 dpf *dmist*^{i8/i8} and *dmist*^{+/+} siblings. Z-score calculated by subtracting mean expression and normalising by the standard deviation across all expressed transcripts. Data are mean \pm SEM for 3 independent biological replicates. ** $p < 0.01$, Student's t-test.

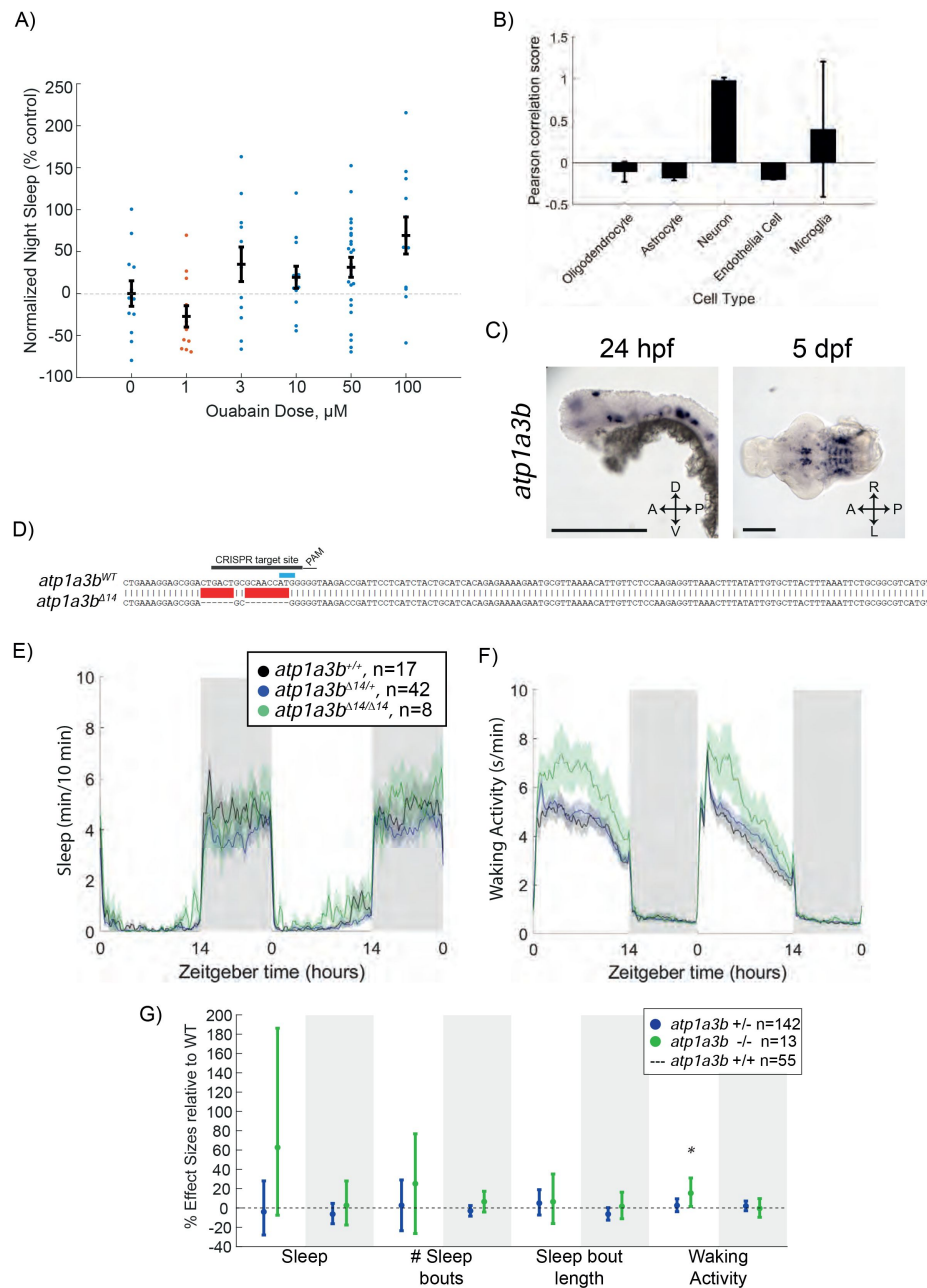


Figure S5.

Ouabain dose curve and effects of *atp1a3b* mutation on behaviour.

A) Dose response curve of ouabain's effects on sleep at night, shown as mean \pm SEM and normalized to the DMSO control. Each data point represents a single fish.

B) Pearson rank correlation of canonical cell-type markers with *Atp1a3a_Mm* shows high co-expression with neuronal markers compared to astroglial and endothelial cell markers. Data are mean \pm SEM.

C) *In situ* hybridisation of *atp1a3a* at 24 hpf (whole animal) and 5 dpf brain (ventral view). Anterior is to the left. Scale bar = 0.5 mm (24 hpf); 0.1 mm (5 dpf).

D) CRISPR-Cas9 targeting of *atp1a3b* resulted in a 14 bp deletion that eliminates the start codon (blue). Guide RNA target sequence and PAM sequence are shown as black bars. The sequence that is deleted in the mutant is indicated with a red bar.

E-F) Representative single behavioural experiment showing *atp1a3b* ^{$\Delta 14/\Delta 14$} mutants have increased daytime waking activity but normal sleep patterns.

G) Data from 2 independent experiments combined with a linear mixed effects model. Plotted are the genotype effect sizes (95% confidence interval) for each parameter relative to wild type (dotted line) for each genotype. Shading indicates day (white) and night (grey). n indicates the number of animals. P-values are assigned by an F-test on the fixed effects coefficients from the linear mixed effects model relative to *atp1a3b*^{+/+} animals. * $p < 0.05$.

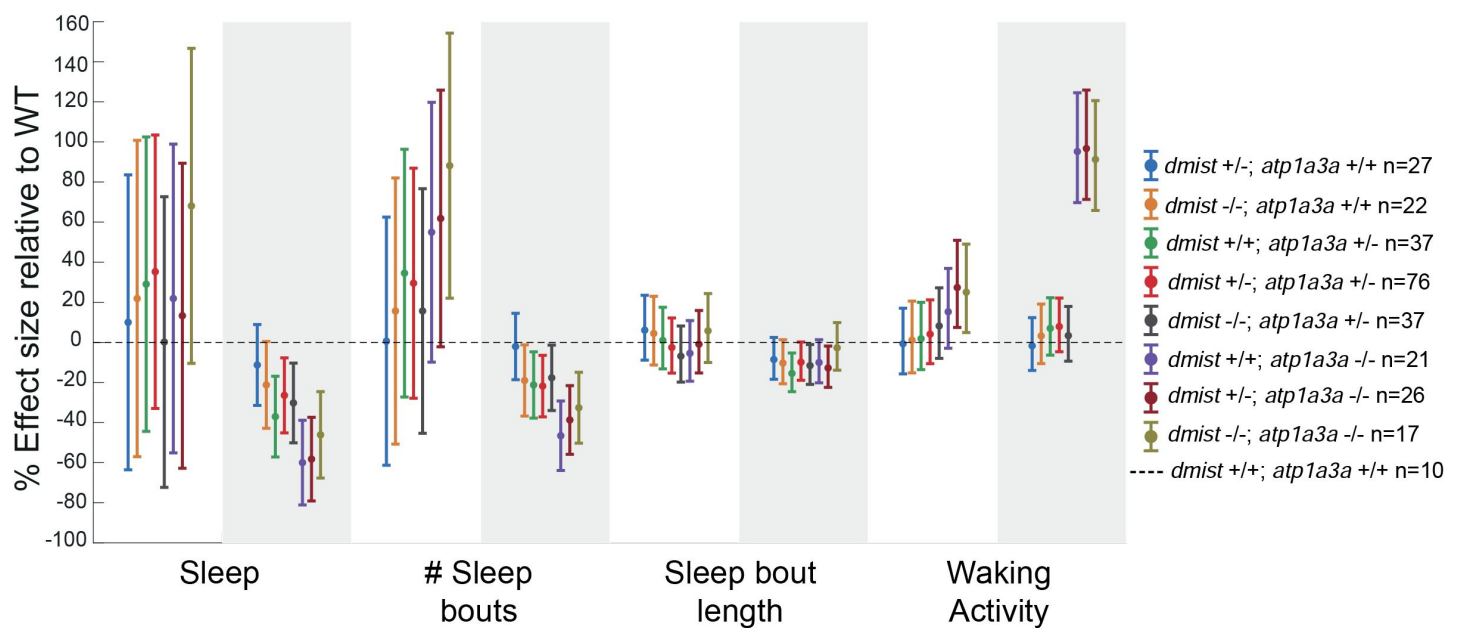


Figure S6.

Sleep effects in *dmist*^{-/-}; *atp1a3a*^{-/-} double mutants are non-additive.

Combining 3 independent experiments with a linear mixed effects model reveals that the effects of loss of function *dmist* and *atp1a3a* mutations are non-additive. Plotted are the genotype effect sizes (95% confidence interval) for each parameter relative to wild type for each genotype. Shading indicates day (white) and night (grey). n indicates the number of animals.

References

- Aday A.W., Zhu L.J., Lakshmanan A., Wang J., Lawson N.D (2011) **Identification of cis regulatory features in the embryonic zebrafish genome through large-scale profiling of H3K4me1 and H3K4me3 binding sites** *Dev. Biol* **357**:450–462 <https://doi.org/10.1016/j.ydbio.2011.03.007>
- Allebrandt K. V., Amin N., Müller-Myhsok B., Esko T., Teder-Laving M., Azevedo R.V.D.M., Hayward C., van Mill J., Vogelzangs N., Green E.W., et al. (2013) **A KATP channel gene effect on sleep duration: from genome-wide association studies to function in *Drosophila*** *Mol. Psychiatry* **18**:122–132 <https://doi.org/10.1038/mp.2011.142>
- Azarias G., Kruusmägi M., Connor S., Akkuratov E.E., Liu X.L., Lyons D., Brismar H., Broberger C., Aperia A (2013) **A specific and essential role for Na,K-ATPase $\alpha 3$ in neurons co-expressing $\alpha 1$ and $\alpha 3$** *J. Biol. Chem* **288**:2734–2743 <https://doi.org/10.1074/jbc.M112.425785>
- Barlow I.L., Rihel J (2017) **Zebrafish sleep: from geneZZZ to neuronZZZ** *Curr. Opin. Neurobiol* **44**:65–71 <https://doi.org/10.1016/j.conb.2017.02.009>
- Bushey D., Huber R., Tononi G., Cirelli C (2007) ***Drosophila* Hyperkinetic mutants have reduced sleep and impaired memory** *J. Neurosci* **27**:5384–93 <https://doi.org/10.1523/JNEUROSCI.0108-07.2007>
- Canfield V.A., Loppin B., Thisse B., Thisse C., Postlethwait J.H., Mohideen M.-A.P., Rajarao S.J.R., Levenson R (2002) **Na,K-ATPase α and β subunit genes exhibit unique expression patterns during zebrafish embryogenesis** *Mech. Dev* **116**:51–59 [https://doi.org/10.1016/S0925-4773\(02\)00135-1](https://doi.org/10.1016/S0925-4773(02)00135-1)
- Chang J.T., Lowery L.A., Sive H (2012) **Multiple roles for the Na,K-ATPase subunits, *Atp1a1* and *Fxyd1*, during brain ventricle development** *Dev. Biol* **368**:312–22 <https://doi.org/10.1016/j.ydbio.2012.05.034>
- Chemelli R.M., Willie J.T., Sinton C.M., Elmquist J.K., Scammell T., Lee C., Richardson J.A., Clay Williams S., Xiong Y., Kisanuki Y., et al. (1999) **Narcolepsy in orexin knockout mice: Molecular genetics of sleep regulation** *Cell* **98**:437–451 [https://doi.org/10.1016/S0092-8674\(00\)81973-X](https://doi.org/10.1016/S0092-8674(00)81973-X)
- Chew G.-L., Pauli A., Rinn J.L., Regev A., Schier A.F., Valen E (2013) **Ribosome profiling reveals resemblance between long non-coding RNAs and 5' leaders of coding RNAs** *Development* **140**:2828–34 <https://doi.org/10.1242/dev.098343>
- Chiu C.N., Rihel J., Lee D.A., Singh C., Mosser E.A., Chen S., Sapin V., Pham U., Engle J., Niles B.J., et al. (2016) **A Zebrafish Genetic Screen Identifies Neuromedin U as a Regulator of Sleep/Wake States** *Neuron* **89**:842–856 <https://doi.org/10.1016/j.neuron.2016.01.007>
- Cirelli C (2009) **The genetic and molecular regulation of sleep: from fruit flies to humans** *Nat. Rev. Neurosci* **10**:549–60 <https://doi.org/10.1038/nrn2683>
- Cirelli C., Bushey D., Hill S., Huber R., Kreber R., Ganetzky B., Tononi G (2005) **Reduced sleep in *Drosophila* Shaker mutants** *Nature* **434**:1087–1092 <https://doi.org/10.1038/nature03486>

- Clapcote S.J., Duffy S., Xie G., Kirshenbaum G., Bechard A.R., Schack V.R., Petersen J., Sinai L., Saab B.J., Lerch J.P., et al. (2009) **Mutation I810N in the $\alpha 3$ isoform of Na⁺,K⁺-ATPase causes impairments in the sodium pump and hyperexcitability in the CNS** *Proc. Natl. Acad. Sci. U. S. A* **106**:14085–14090 <https://doi.org/10.1073/pnas.0904817106>
- Clausen M. V., Hilbers F., Poulsen H (2017) **The Structure and Function of the Na,K- ATPase Isoforms in Health and Disease** *Front. Physiol* **8** <https://doi.org/10.3389/fphys.2017.00371>
- Crambert G., Fuzesi M., Garty H., Karlsh S., Geering K (2002) **Phospholemman (FXYP1) associates with Na,K-ATPase and regulates its transport properties** *Proc. Natl. Acad. Sci. U. S. A* **99**:11476–81 <https://doi.org/10.1073/pnas.182267299>
- Damulewicz M., Rosato E., Pyza E (2013) **Circadian regulation of the Na⁺/K⁺- ATPase alpha subunit in the visual system is mediated by the pacemaker and by retina photoreceptors in *Drosophila melanogaster*** *PLoS One* **8**
- Dashti H.S., Jones S.E., Wood A.R., Lane J.M., van Hees V.T., Wang H., Rhodes J.A., Song Y., Patel K., Anderson S.G., et al. (2019) **Genome-wide association study identifies genetic loci for self-reported habitual sleep duration supported by accelerometer-derived estimates** *Nat Commun* **10**
- De Carvalho Aguiar P., Sweadner K.J., Penniston J.T., Zaremba J., Liu L., Caton M., Linazasoro G., Borg M., Tijssen M.A.J., Bressman S.B., et al (2004) **Mutations in the Na⁺/K⁺-ATPase $\alpha 3$ gene ATP1A3 are associated with rapid-onset dystonia parkinsonism** *Neuron* **43**:169–175 <https://doi.org/10.1016/j.neuron.2004.06.028>
- Despa S., Tucker A.L., Bers D.M (2008) **Phospholemman-mediated activation of Na/K-ATPase limits [Na]_i and inotropic state during β -adrenergic stimulation in mouse ventricular myocytes** *Circulation* **117**:1849–1855 <https://doi.org/10.1161/CIRCULATIONAHA.107.754051>
- Ding F., O'donnell J., Xu Q., Kang N., Goldman N., Nedergaard M (2016) **Changes in the composition of brain interstitial ions control the sleep-wake cycle** *Science (80-.)* **352**:550–555 <https://doi.org/10.1126/science.aad4821>
- Doğanli C., Beck H.C., Ribera A.B., Oxvig C., Lykke-Hartmann K. (2013) **$\alpha 3$ Na⁺/K⁺- ATPase deficiency causes brain ventricle dilation and abrupt embryonic motility in zebrafish** *J. Biol. Chem* **288**:8862–8874 <https://doi.org/10.1074/jbc.M112.421529>
- Dostanic I., Schultz Jel J., Lorenz J. N., Lingrel J. B. (2004) **The alpha 1 isoform of Na,K-ATPase regulates cardiac contractility and functionally interacts and co-localizes with the Na/Ca exchanger in heart** *J Biol Chem* **279**:54053–61
- Douglas C.L., Vyazovskiy V., Southard T., Chiu S.-Y., Messing A., Tononi G., Cirelli C (2007) **Sleep in *Kcna2* knockout mice** *BMC Biol* **5** <https://doi.org/10.1186/1741-7007-5-42>
- Ewart H.S., Klip A (1995) **Hormonal regulation of the Na(+)-K(+)-ATPase: mechanisms underlying rapid and sustained changes in pump activity** *Am J Physiol* **269**:C295–311
- Feschenko M.S., Donnet C., Wetzel R.K., Asinowski N.K., Jones L.R., Sweadner K.J (2003) **Phospholemman, a single-span membrane protein, is an accessory protein of Na,K-ATPase in cerebellum and choroid plexus** *J. Neurosci* **23**:2161–2169 <https://doi.org/10.1523/jneurosci.23-06-02161.2003>

- Funato H., Miyoshi C., Fujiyama T., Kanda T., Sato M., Wang Z., Ma J., Nakane S., Tomita J., Ikkyu A., et al. (2016) **Forward-genetics analysis of sleep in randomly mutagenized mice** *Nature* **539**:378–383 <https://doi.org/10.1038/nature20142>
- Gagnon J.A., Valen E., Thyme S.B., Huang P., Ahkmetova L., Pauli A., Montague T.G., Zimmerman S., Richter C., Schier A.F (2014) **Efficient Mutagenesis by Cas9 Protein-Mediated Oligonucleotide Insertion and Large-Scale Assessment of Single- Guide RNAs** *PLoS One* **9** <https://doi.org/10.1371/journal.pone.0098186>
- Gandhi A. V., Mosser E.A., Oikonomou G., Prober D.A (2015) **Melatonin Is Required for the Circadian Regulation of Sleep** *Neuron* **85**:1–7 <https://doi.org/10.1016/j.neuron.2015.02.016>
- Geering K., Béguin P., Garty H., Karlsh S., Füzesi M., Horisberger J.D., Crambert G (2003) **FXD proteins: New tissue- and isoform-specific regulators of Na,K-ATPase** *Annals of the New York Academy of Sciences* :388–394 <https://doi.org/10.1111/j.1749-6632.2003.tb07219.x>
- Giraldez A.J., Mishima Y., Rihel J., Grocock R.J., Van Dongen S., Inoue K., Enright A.J., Schier A.F. (2006) **Zebrafish MiR-430 promotes deadenylation and clearance of maternal mRNAs** *Science* **312**:75–79 <https://doi.org/10.1126/science.1122689>
- Grunwald H.A., Gantz V.M., Poplawski G., Xu X.R.S., Bier E., Cooper K.L (2019) **Super-Mendelian inheritance mediated by CRISPR-Cas9 in the female mouse germline** *Nature* <https://doi.org/10.1038/s41586-019-0875-2>
- Heinzen E.L., Arzimanoglou A., Brashear A., Clapcote S.J., Gurrieri F., Goldstein D.B., Jóhannesson S.H., Mikati M.A., Neville B., Nicole S., et al. (2014) **Distinct neurological disorders with ATP1A3 mutations** *Lancet. Neurol* **13**:503–14 [https://doi.org/10.1016/S1474-4422\(14\)70011-0](https://doi.org/10.1016/S1474-4422(14)70011-0)
- Heinzen E.L., Swoboda K.J., Hitomi Y., Gurrieri F., De Vries B., Tiziano F.D., Fontaine B., Walley N.M., Heavin S., Panagiotakaki E., et al. (2012) **De novo mutations in ATP1A3 cause alternating hemiplegia of childhood** *Nat. Genet* **44**:1030–1034 <https://doi.org/10.1038/ng.2358>
- Hoffman E.J., Turner K.J., Fernandez J.M., Cifuentes D., Ghosh M., Ijaz S., Jain R.A., Kubo F., Bill B.R., Baier H., et al. (2016) **Estrogens Suppress a Behavioral Phenotype in Zebrafish Mutants of the Autism Risk Gene, CNTNAP2** *Neuron* **89**:725–733 <https://doi.org/10.1016/j.neuron.2015.12.039>
- Hunanyan A.S., Fainberg N.A., Linabarger M., Arehart E., Leonard A.S., Adil S.M., Helseth A.R., Swearingen A.K., Forbes S.L., Rodriguiz R.M., et al. (2015) **Knock-in mouse model of alternating hemiplegia of childhood: Behavioral and electrophysiologic characterization** *Epilepsia* **56**:82–93 <https://doi.org/10.1111/epi.12878>
- Iannacone M.J., Beets I., Lopes L.E., Churgin M.A., Fang-Yen C., Nelson M.D., Schoofs L., Raizen D.M (2017) **The RFamide receptor DMSR-1 regulates stress-induced sleep in C. elegans** *Elife* **6** <https://doi.org/10.7554/eLife.19837>
- Ikeda K., Satake S., Onaka T., Sugimoto H., Takeda N., Imoto K., Kawakami K (2013) **Enhanced inhibitory neurotransmission in the cerebellar cortex of Atp1a3-deficient heterozygous mice** *J. Physiol* **591**:3433–3449 <https://doi.org/10.1113/jphysiol.2012.247817>

- Jansen P.R., Watanabe K., Stringer S., Skene N., Bryois J., Hammerschlag A.R., de Leeuw C.A., Benjamins J.S., Muñoz-Manchado A.B., Nagel M., et al. (2019) **Genome-wide analysis of insomnia in 1,331,010 individuals identifies new risk loci and functional pathways** *Nat. Genet* **51**:394–403 <https://doi.org/10.1038/s41588-018-0333-3>
- Jao L.-E., Wente S.R., Chen W (2013) **Efficient multiplex biallelic zebrafish genome editing using a CRISPR nuclease system** *Proc. Natl. Acad. Sci. U. S. A* **110**:13904–9 <https://doi.org/10.1073/pnas.1308335110>
- Johnson L.S., Eddy S.R., Portugaly E (2010) **Hidden Markov model speed heuristic and iterative HMM search procedure** *BMC Bioinformatics* **11** <https://doi.org/10.1186/1471-2105-11-431>
- Joiner W.J (2016) **Unraveling the Evolutionary Determinants of Sleep** *Curr. Biol* **26**:R1073–R1087 <https://doi.org/10.1016/j.cub.2016.08.068>
- Jones S.E., van Hees V.T., Mazzotti D.R., Marques-Vidal P., Sabia S., van der Spek A., Dashti H.S., Engmann J., Kocavska D., Tyrrell J., et al. (2019) **Genetic studies of accelerometer-based sleep measures yield new insights into human sleep behaviour** *Nat Commun* **10**
- Jumper J., Evans R., Pritzel A., Green T., Figurnov M., Ronneberger O., Tunyasuvunakool K., Bates R., Zidek A., Potapenko A., Bridgland A., Meyer C., Kohl S. A. A., Ballard A. J., Cowie A., Romera-Paredes B., Nikolov S., Jain R., Adler J., Back T., Petersen S., Reiman D., Clancy E., Zielinski M., Steinegger M., Pacholska M., Berghammer T., Bodenstein S., Silver D., Vinyals O., Senior A. W., Kavukcuoglu K., Kohli P., Hassabis D. (2021) **Highly accurate protein structure prediction with AlphaFold** *Nature* **596**:583–89
- Kansagra S., Ghusayni R., Kherallah B., Gunduz T., McLean M., Prange L., Kravitz R.M., Mikati M.A (2019) **Polysomnography findings and sleep disorders in children with alternating hemiplegia of childhood** *J. Clin. Sleep Med* **15**:65–70 <https://doi.org/10.5664/jcsm.7572>
- Katoh K., Toh H (2010) **Parallelization of the MAFFT multiple sequence alignment program** *Bioinformatics* <https://doi.org/10.1093/bioinformatics/btq224>
- Kempf A., Song S.M., Talbot C.B., Miesenböck G (2019) **A potassium channel β - subunit couples mitochondrial electron transport to sleep** *Nature* **568**:230–234 <https://doi.org/10.1038/s41586-019-1034-5>
- Kimmel C.B., Ballard W.W., Kimmel S.R., Ullmann B., Schilling T.F (1995) **Stages of embryonic development of the zebrafish** *Dev. Dyn* **203**:253–310 <https://doi.org/10.1002/aja.1002030302>
- Kirshenbaum G.S., Clapcote S.J., Duffy S., Burgess C.R., Petersen J., Jarowek K.J., Yücel Y.H., Cortez M.A., Snead O.C., Vilsen B., et al. (2011) **Mania-like behavior induced by genetic dysfunction of the neuron-specific Na^+ , K^+ -ATPase $\alpha 3$ sodium pump** *Proc. Natl. Acad. Sci. U. S. A* **108**:18144–18149 <https://doi.org/10.1073/pnas.1108416108>
- Koh K., Joiner W.J., Wu M.N., Yue Z., Smith C.J., Sehgal A (2009) **Identification of SLEEPLESS, a novel sleep promoting factor** *Science* <https://doi.org/10.1126/science.1155942>
- Kristensen A.S., Andersen J., Jorgensen T.N., Sorensen L., Eriksen J., Loland C.J., Stromgaard K., Gether U (2011) **SLC6 neurotransmitter transporters: Structure, function, and regulation** *Pharmacol. Rev* **63**:585–640 <https://doi.org/10.1124/pr.108.000869>

- Kwan K.M., Fujimoto E., Grabher C., Mangum B.D., Hardy M.E., Campbell D.S., Parant J.M., Yost H.J., Kanki J.P., Chien C.-B (2007) **The Tol2kit: a multisite gateway- based construction kit for Tol2 transposon transgenesis constructs** *Dev. Dyn* **236**:3088–99 <https://doi.org/10.1002/dvdy.21343>
- Lane J.M., Jones S.E., Dashti H.S., Wood A.R., Aragam K.G., van Hees V.T., Strand L.B., Winsvold B.S., Wang H., Bowden J., et al. (2019) **Biological and clinical insights from genetics of insomnia symptoms** *Nat Genet* **51**:387–393
- Lee D.A., Andreev A., Truong T. V., Chen A., Hill A.J., Oikonomou G., Pham U., Hong Y.K., Tran S., Glass L., et al. (2017) **Genetic and neuronal regulation of sleep by neuropeptide VF** *Elife* **6** <https://doi.org/10.7554/eLife.25727>
- Lek M., Karczewski K.J., Minikel E. V., Samocha K.E., Banks E., Fennell T., O'Donnell- Luria A.H., Ware J.S., Hill A.J., Cummings B.B., et al. (2016) **Analysis of protein- coding genetic variation in 60,706 humans** *Nature* **536**:285–291 <https://doi.org/10.1038/nature19057>
- Lenz O., Xiong J., Nelson M.D., Raizen D.M., Williams J.A (2015) **FMRamide signaling promotes stress-induced sleep in Drosophila** *Brain. Behav. Immun* **47**:141–148 <https://doi.org/10.1016/j.bbi.2014.12.028>
- Li SB, Damonte VM, Chen C, Wang GX, Kebschull JM, Yamaguchi H, Bian WJ, Purmann C, Pattni R, Urban AE, Mourrain P, Kauer JA, Scherrer G, de Lecea L (2022) **Hyperexcitable arousal circuits drive sleep instability during aging** *Science* **375**
- Lin L, Faraco J, Li R, Kadotani H, Rogers W, Lin X, Qiu X, de Jong P.J, Nishino S, Mignot E., et al. (1999) **The sleep disorder canine narcolepsy is caused by a mutation in the hypocretin (orexin) receptor 2 gene** *Cell* **98**:365–76 [https://doi.org/10.1016/S0092-8674\(00\)81965-0](https://doi.org/10.1016/S0092-8674(00)81965-0)
- Love M.I., Huber W., Anders S (2014) **Moderated estimation of fold change and dispersion for RNA-seq data with DESeq2** *Genome Biol* **15** <https://doi.org/10.1186/s13059-014-0550-8>
- McGrail K.M., Phillips J.M., Sweadner K.J (1991) **Immunofluorescent localization of three Na,K-ATPase isozymes in the rat central nervous system: Both neurons and glia can express more than one Na,K-ATPase** *J. Neurosci* **11**:381–391 <https://doi.org/10.1523/jneurosci.11-02-00381.1991>
- Montague T.G., Cruz J.M., Gagnon J.A., Church G.M., Valen E (2014) **CHOPCHOP: a CRISPR/Cas9 and TALEN web tool for genome editing** *Nucleic Acids Res. gku* <https://doi.org/10.1093/nar/gku410>
- Nakashima A., Kawamoto T., Noshiro M., Ueno T., Doi S., Honda K., Maruhashi T., Noma K., Honma S., Masaki T., et al. (2018) **Dec1 and CLOCK Regulate Na(+)/K(+) ATPase beta1 Subunit Expression and Blood Pressure** *Hypertension* **72**:746–754
- Oikonomou G., Altermatt M., Zhang R. wei, Coughlin G.M., Montz C., Gradinaru V., Prober D.A. (2019) **The Serotonergic Raphe Promote Sleep in Zebrafish and Mice** *Neuron* **103**:686–701 <https://doi.org/10.1016/j.neuron.2019.05.038>
- Palagini L., Domschke K., Benedetti F., Foster R.G., Wulff K., Riemann D (2019) **Developmental pathways towards mood disorders in adult life: Is there a role for sleep disturbances? J. Affect. Disord** **243**:121–132 <https://doi.org/10.1016/j.JAD.2018.09.011>

- Pauli A., Valen E., Lin M.F., Garber M., Vastenhouw N.L., Levin J.Z., Fan L., Sandelin A., Rinn J.L., Regev A., et al. (2012) **Systematic identification of long noncoding RNAs expressed during zebrafish embryogenesis** *Systematic identification of long noncoding RNAs expressed during zebrafish embryogenesis* :577–591 <https://doi.org/10.1101/gr.133009.111>
- Pauli A., Valen E., Schier A.F (2015) **Identifying (non-)coding RNAs and small peptides: Challenges and opportunities** *BioEssays* **37**:103–112 <https://doi.org/10.1002/bies.201400103>
- Pavlovic D., Fuller W., Shattock M.J (2013) **Novel regulation of cardiac Na pump via phospholemman** *J. Mol. Cell. Cardiol* **61**:83–93 <https://doi.org/10.1016/j.yjmcc.2013.05.002>
- Peyron C., Faraco J., Rogers W., Ripley B., Overeem S., Charnay Y., Nevsimalova S., Aldrich M., Reynolds D., Albin R., et al. (2000) **A mutation in a case of early onset narcolepsy and a generalized absence of hypocretin peptides in human narcoleptic brains** *Nat Med* **6**:991–997
- Price E. M., Lingrel J. B. (1988) **Structure-function relationships in the Na,K-ATPase alpha subunit: site-directed mutagenesis of glutamine-111 to arginine and asparagine- 122 to aspartic acid generates a ouabain-resistant enzyme** *Biochemistry* **27**:8400–8
- Prober D. a, Rihel J., Onah A. a, Sung R.-J., Schier A.F (2006) **Hypocretin/orexin overexpression induces an insomnia-like phenotype in zebrafish** *J. Neurosci* **26**:13400–10 <https://doi.org/10.1523/JNEUROSCI.4332-06.2006>
- Reichert S., Pavón Arocas O., Rihel J (2019) **The Neuropeptide Galanin Is Required for Homeostatic Rebound Sleep following Increased Neuronal Activity** *Neuron* **104**:370–384 <https://doi.org/10.1016/j.neuron.2019.08.010>
- Rihel J., Prober D. a, Arvanites A., Lam K., Zimmerman S., Jang S., Haggarty S.J., Kokel D., Rubin L.L., Peterson R.T., et al. (2010) **Zebrafish behavioral profiling links drugs to biological targets and rest/wake regulation** *Science* **327**:348–51 <https://doi.org/10.1126/science.1183090>
- Rihel J., Schier A.F (2013) **Sites of action of sleep and wake drugs: insights from model organisms** *Curr. Opin. Neurobiol* **23**:831–40 <https://doi.org/10.1016/j.conb.2013.04.010>
- Salles P.A., Mata I.F., Brunger T., Lal D., Fernandez H.H (2021) **ATP1A3-Related Disorders: An Ever-Expanding Clinical Spectrum** *Front Neurol* **12**
- Sakurai T (2013) **Orexin deficiency and narcolepsy** *Curr. Opin. Neurobiol* **23**:760–766 <https://doi.org/10.1016/j.conb.2013.04.007>
- Sehgal A., Mignot E (2011) **Genetics of sleep and sleep disorders** *Cell* **146**:194–207 <https://doi.org/10.1016/j.cell.2011.07.004>
- Shah A.N., Davey C.F., Whitebirch A.C., Miller A.C., Moens C.B (2015) **Rapid reverse genetic screening using CRISPR in zebrafish** *Nat. Methods* **12**:535–540 <https://doi.org/10.1038/nmeth.3360>
- Shankaran S.S., Dahlem T.J., Bisgrove B.W., Yost H.J., Tristani-Firouzi M (2017) **CRISPR/Cas9-Directed Gene Editing for the Generation of Loss-of-Function Mutants in High-Throughput Zebrafish F 0 Screens, in: Current Protocols in Molecular Biology** :31–31 <https://doi.org/10.1002/cpmb.42>

- Singh C., Oikonomou G., Prober D.A (2015) **Norepinephrine is required to promote wakefulness and for hypocretin-induced arousal in zebrafish** *Elife* 4
- Singh C., Rihel J., Prober D.A (2017) **Neuropeptide Y Regulates Sleep by Modulating Noradrenergic Signaling** *Curr. Biol* 27:3796–3811 <https://doi.org/10.1016/j.CUB.2017.11.018>
- Sivasubbu S., Balciunas D., Amsterdam A., Ekker S.C. (2007) **Insertional mutagenesis strategies in zebrafish** <https://doi.org/10.1186/gb-2007-8-s1-s9>
- Sugimoto H., Ikeda K., Kawakami K (2014) **Heterozygous mice deficient in Atp1a3 exhibit motor deficits by chronic restraint stress** *Behav. Brain Res* 272:100–110 <https://doi.org/10.1016/j.bbr.2014.06.048>
- Sweadner K.J., Rael E (2000) **The FXYD gene family of small ion transport regulators or channels: cDNA sequence, protein signature sequence, and expression** *Genomics* 68:41–56 <https://doi.org/10.1006/geno.2000.6274>
- Therien A.G., Blostein R. (2000) **Mechanisms of sodium pump regulation** *Am J Physiol Cell Physiol* 279:C541–566
- Thisse B., Pflumio S., Fürthauer M., Loppin B., Heyer V., Degrave A., Woehl R., Lux A., Steffan T., Charbonnier X.Q., Thisse C. (2001) **Expression of the zebrafish genome during embryogenesis (NIH R01 RR15402)**
- Thisse C., Thisse B (2008) **High-resolution in situ hybridization to whole-mount zebrafish embryos** *Nat. Protoc* 3:59–69 <https://doi.org/10.1038/nprot.2007.514>
- Toda H., Williams J.A., Gulledge M., Sehgal A (2019) **A sleep-inducing gene, nemuri, links sleep and immune function in Drosophila** *Science* 363:509–515 <https://doi.org/10.1126/science.aat1650>
- Ulitsky I., Shkumatava A., Jan C.H., Sive H., Bartel D.P (2011) **Conserved function of lincRNAs in vertebrate embryonic development despite rapid sequence evolution** *Cell* 147:1537–1550 <https://doi.org/10.1016/j.cell.2011.11.055>
- Varshney G.K., Lu J., Gildea D.E., Huang H., Pei W., Yang Z., Huang S.C., Schoenfeld D., Pho N.H., Casero D., et al. (2013) **A large-scale zebrafish gene knockout resource for the genome-wide study of gene function** *Genome Res* 23:727–35 <https://doi.org/10.1101/gr.151464.112>
- Villalba A., Coll O., Gebauer F (2011) **Cytoplasmic polyadenylation and translational control** *Curr. Opin. Genet. Dev* 21:452–457 <https://doi.org/10.1016/j.gde.2011.04.006>
- Wilkinson R.N., Elworthy S., Ingham P.W., van Eeden F.J.M. (2013) **A method for high-throughput PCR-based genotyping of larval zebrafish tail biopsies** *Biotechniques* 55:314–316 <https://doi.org/10.2144/000114116>
- Wittkopp N., Huntzinger E., Weiler C., Saulière J., Schmidt S., Sonawane M., Izaurralde E (2009) **Nonsense-mediated mRNA decay effectors are essential for zebrafish embryonic development and survival** *Mol Cell Biol* 29:3517–28
- Wu M., Robinson J.E., Joiner W.J (2014) **SLEEPLESS Is a Bifunctional Regulator of Excitability and Cholinergic Synaptic Transmission** *Curr. Biol* 24:621–629 <https://doi.org/10.1016/j.cub.2014.02.026>

Wu R.S., Lam I.I., Clay H., Duong D.N., Deo R.C., Coughlin S.R (2018) **A Rapid Method for Directed Gene Knockout for Screening in G0 Zebrafish** *Dev. Cell* **46**:112–125 <https://doi.org/10.1016/j.devcel.2018.06.003>

Zhang Y., Chen K., Sloan S.A., Bennett M.L., Scholze A.R., O’Keeffe S., Phatnani H.P., Guarnieri P., Caneda C., Ruderisch N., et al. (2014) **An RNA-sequencing transcriptome and splicing database of glia, neurons, and vascular cells of the cerebral cortex** *J. Neurosci* **34**:11929–11947 <https://doi.org/10.1523/JNEUROSCI.1860-14.2014>

Author information

Ida L. Barlow

Department of Cell and Developmental Biology, University College London, UK; MRC London Institute for Medical Sciences, Imperial College London, UK
ORCID iD: [0000-0003-1046-9606](https://orcid.org/0000-0003-1046-9606)

Eirinn Mackay

Department of Cell and Developmental Biology, University College London, UK; Sainsbury Wellcome Centre for Neural Circuits and Behaviour, University College London, UK
ORCID iD: [0000-0003-1436-2259](https://orcid.org/0000-0003-1436-2259)

Emily Wheeler

Department of Cell and Developmental Biology, University College London, UK; MRC centre for Reproductive Health, University of Edinburgh, UK

Aimee Goel

Department of Cell and Developmental Biology, University College London, UK;

Sumi Lim

Department of Cell and Developmental Biology, University College London, UK;
ORCID iD: [0000-0002-1614-9753](https://orcid.org/0000-0002-1614-9753)

Steve Zimmerman

Department of Molecular and Cellular Biology, Harvard University, USA

Ian Woods

Ithaca College, New York, USA

David A. Prober

Division of Biology and Biological Engineering, California Institute of Technology, Pasadena, USA
ORCID iD: [0000-0002-7371-4675](https://orcid.org/0000-0002-7371-4675)

Jason Rihel

Department of Cell and Developmental Biology, University College London, UK;
For correspondence: j.rihel@ucl.ac.uk
ORCID iD: [0000-0003-4067-2066](https://orcid.org/0000-0003-4067-2066)

Editors

Reviewing Editor

Ying-Hui Fu

University of California, San Francisco, United States of America

Senior Editor

Didier Stainier

Max Planck Institute for Heart and Lung Research, Germany

Reviewer #1 (Public Review):

Barlow et al performed a viral insertion screen in larval zebrafish for sleep mutants. They identify a mutant named dreammist (dmist) that displayed defects in sleep, namely, decreased sleep both day and night, accompanied by increased activity. They find that dmist encodes a previously uncharacterized single-pass transmembrane protein that shows structural similarity to Fxyd1, a Na⁺K⁺-ATPase regulator. Disruption of fxyd1 or atp1a3a, a Na⁺,K⁺-ATPase alpha-3 subunit, decreased night-time sleep. By staining for sodium levels, the authors uncover a global increase of sodium in both dmist and atp1a3a mutants following PTZ treatment, consistent with defects in Na⁺K⁺-ATPase function. These genetic data from multiple mutant lines help establish the importance of sodium and/or potassium homeostasis in sleep regulation.

The conclusions of this paper are mostly well supported by data, with the following strengths and weaknesses as described below.

Strengths:

Elegant use of CRISPR knockout methods to disrupt multiple genes that help establish the importance of regulating Na⁺K⁺-ATPase function in sleep.

Data are mostly clearly presented.

Double mutant analysis of dmist and atp1a3a help establish an epistatic relationship between these proteins.

Weaknesses:

The authors emphasize the role of increased cellular sodium, but equally plausibly, the phenotypes could be due to decreased cellular potassium. The potassium channel shaker has been previously identified as a critical sleep regulator in *Drosophila*.

Although the increased sleep rebound after PTZ treatment in the dmist mutant is interesting, I find it difficult to understand, especially in the context of the dmist mutant having decreased sleep.

The similar phenotype between dmist and Fxyd1 in sleep reduction yet very different expression patterns, with dmist being mostly neuronal while fxyd1 being mostly non-neuronal, raise many possible questions: 1) are the sleep phenotypes due to neuronal Na/K imbalance? Or 2) Are the sleep phenotypes due to extracellular Na/K imbalance? Or 3) both? Some feasible experiments may help achieve a better mechanistic understanding of the observed sleep defects.

Reviewer #2 (Public Review):

Barlow and colleagues describe a role for the Na⁺/K⁺ pump in sleep/wake regulation. They discovered this role starting with a forward genetic screen in which they tested a biased sample of virus insertion fish lines for sleep phenotypes. They found an insertion in a gene they named dreammist, which is homologous to the gene FXYD1 encoding single membrane-

pass modifiers of Na/K pumps. They go on to show that genetic manipulations of either FXD1 or the Na/K pump also reduce sleep. They use pharmacology and sleep deprivation experiments to provide further evidence that the Na/K pump regulates intracellular sodium and rebound sleep. This study provides additional evidence for the important role of membrane excitability in sleep regulation (prior studies have implicated K⁺ channel subunits as well as a sodium leak ion channel).

The study is well done and convincing with regard to its major conclusions. I had some minor comments/questions, which they properly addressed in their revision and rebuttal.

Author Response

The following is the authors' response to the original reviews.

We thank the reviewers for their comments. We have now addressed all the comments in a revised version of the manuscript, which we believe has strengthened our paper.

1. *Introduction LINE 60: the authors cite Funato et al 2016 as the paper first describing a role for SIK3 in sleep regulation. In fact, the role for this kinase was first identified nearly a decade earlier in C. elegans (Van der Linden et al, Genetics 2008 PMID 18832350).*

Thank you for pointing us to this reference. Van der Linden et al. demonstrated that the *C. elegans* homolog of SIK3 (KIN-29) regulates satiety quiescence, in which worms stop moving following feeding on high quality food. However, as pointed out in Trojanowski and Raizen "Call it Worm Sleep" (2016), not all of the behavioral criteria for sleep has been applied to *C. elegans* satiety quiescence, and we cannot find any references that unequivocally demonstrate satiety quiescence is a sleep state. As McClanahan et al., (2020) show, quiescent states following mild sensory arousal do not fulfill the sleep criteria of changes in arousal threshold and homeostatic regulation, so not all quiescent states in *C. elegans* are sleep. Then again Grubbs et al, 2020 does demonstrate that KIN29 regulates both developmentally timed and stress induced sleep states in worms, suggesting that the observations in Van der Linden were ahead of its time and these behavioral states are possibly inter-related. We believe, though, that our line "the roles of... SIK3 kinase in modulating sleep homeostasis in mice (Funato et al. 2016) were identified in genetic screens" remains accurate.

1. *Introduction LINE 71: remove the word "known" from "...while some known human sleep/wake regulators, such as the..."*

Good idea. Done.

1. *I was confused regarding Supplemental data 1 describing the genes they targeted with their forward genetic screen. Am I understanding correctly from the "Summary stats" tab that 702 fish lines with virus insertions were screened behaviorally? In Figure S1, it looks like about 60 are shown in the histograms but in the text (in the Discussion) they say 25 were screened. Were all the genes listed under the Excel tabs (GPCRs, channels, etc) tested? Or was just a subset tested? Where are the sleep data for these lines? Negative results may be relevant to their manuscript since they listed (tested??) a number of ion channel genes under tab "channels" which appear to NOT have a sleep phenotype.*

We apologize for the confusion on these points. As highlighted in the legend to Supplementary Figure S1, we had planned a screening strategy with the following pipeline: Candidate mammalian gene → Zebrafish ortholog → ID viral insertion from "Zenemark" library → grow viral insertion lines from frozen sperm → phenotype F3 heterozygous and homozygous mutant generation. Unfortunately, the company, Znomics, which held the

Zenemark library, could not reliably reconstitute the correct live fish from the sperm library, and of the 702 lines we planned to screen, we could only screen 26 (25 was a typo) lines. We treated heterozygous and homozygous animals for each line independently, for a total of 52 screened lines in the histograms.

To make this clearer, we have edited the main text as follows (lines 104-105): “For screening, we identified zebrafish sperm samples from the Zenemark collection (Varshney et al., 2013) that harboured viral insertions in genes of interest and used these samples for in vitro fertilization and the establishment of F2 families, which we were able to obtain for 26 lines.” And lines 111-112: “While most screened heterozygous and homozygous lines had minimal effects on sleep-wake behavioural parameters (Figure S1B-S1C),”

We believe it is important to include the full set of Supplementary Data 1, even though the vast majority of these candidate lines were not tested.

1. *Results LINE 117: remove the word "prominent", which is subjective, from the sentence "...showed a prominent decrease in sleep during the..."*

Good point. Done.

1. *LINE 185-186: did you see any circadian variation in your dmist:GFP protein abundance or localization? Protein trafficking has been described as a mechanism of circadian regulation of excitability.*

For practical reasons, we imaged the membrane localization of Dmist:GFP in plasmid-injected embryos at 90% epiboly, which is about 9 hours after fertilization and when the cells remain large and in a relatively flat epithelium. Thus, we could not follow circadian fluctuations in abundance or localization. For circadian studies, we believe the best method will be to raise an antibody that recognizes Dmist.

1. *LINE 203: does the GFP-tagged Dmist rescue the loss-of-function phenotype? This is relevant to Figure 2E. It is also relevant to the issue of structure-function. If it rescues, then the C-terminus may not be essential to protein function.*

As noted, for practical reasons, we observed Dmist-GFP only transiently at early stages of development, expressed using a strong, ubiquitous promoter. A rescue experiment is a good idea for future experiments, where we carefully control the expression of Dmist in neurons.

1. *LINE 220: explain what you mean by "...consistent with nonsense-mediated decay." and/or give a reference.*

In zebrafish and other species including humans, mutant transcripts that have premature stop codons often undergo “nonsense mediated decay”, whereby the expression levels are largely reduced (Wittkopp et al., 2009). In the zebrafish community, this is often used as secondary evidence of a loss of function mutation, as relatively few antibodies are available to directly observe zebrafish proteins. We have added a reference that describes this phenomenon (Wittkopp et al., 2009).

1. *LINE 225: define "LME model"*

Now reads: “Linear mixed effects (LME).”

1. *LINE 227-229: could the vir/vir phenotype be explained by specific effects on protein structure? could vir/vir be a gain-of-function allele?*

We can't rule this out formally, and *vir/+* animals do show some sleep phenotypes, albeit weaker than those of *vir/vir* animals (Figure 1G). However, it is not uncommon for heterozygous mutants to show significant phenotypes that are weaker than those of their homozygous mutant siblings, and the strong suppression of *dmist* expression by the viral insertion (which is located in the *dmist* intron) is more consistent with a hypomorphic loss-of-function phenotype for the *vir* allele.

1. *LINES 229-230: I don't quite follow the argument for pursuing further studies only of i8/i8. i8/i8 seems to also be a hypomorphic allele based on your qPCR data.*

First, the *dmist* viral line was generated by an insertional mutagenesis method followed by sequencing, and each line has multiple other inserts in a background that does not match the background of the other animals reported in this paper. Second, the *dmist vir* allele is an insertion in the intron, leading to reduced, but not complete loss of expression. In contrast, the *i8* allele was generated on the same background strain as our other existing and newly reported lines. Moreover, our *i8* line is likely a loss-of-function allele and not a hypomorph. Yes, *dmist* expression is reduced in the *i8* allele; however, this is likely due to nonsense mediated decay of *dmist* mRNA. The mutation introduces a frameshift in the *dmist* coding sequence, and as a result the amino acid sequence of the protein is altered after the N-terminal signal sequence.

1. *LINES 241-243: grammar.*

Fixed

1. *LINE 245: define "JackHMMR iterative search"*

We've added the phrase: "and seeding a hidden Markov model iterative search (JackHMMR)"

1. *LINE 246 is missing the word "we" prior to "...found distant homology between..."*

Added

1. *LINE 301: show data demonstrating deviation from Mendelian ratios. Also, comment on meaning of such data (embryonic lethality??).*

We have added this data in the line (301):

"*atp1a3b* mutant larvae were not obtained at Mendelian ratios (55 wild type [52.5 expected], 142 [105] *atp1a3b*+/-, 13 [52.5] *atp1a3b*-/-; $p < 0.0001$, Chi-squared) suggesting some impact on early stages of development leading to lethality."

1. *Discussion LINES 362-372: This paragraph seems to be of only tangential relevance to the paper. Consider removing.*

Our screening strategy was a large-scale reverse genetic screen, but the number of lines was limited by the technical issues described above. We think it is important to mention that the strategy, if employed today, could benefit from newer technologies.

1. *Discussion. Another model is that Dmist and NaK pump have a developmental effect. Arguing against this developmental model is the Oubain expt.*

This is an important point. We've added the line (454:457): "We also cannot exclude a role for *Dmist* and the Na^+/K^+ pump in developmental events that impact sleep, although our

observation that ouabain treatment, which inhibits the pump acutely after early development is complete, also impacts sleep, argues against a developmental role.”

1. *FIGURE 1G: Are these significance cut offs corrected for multiple comparisons?*

Yes, all the data is corrected for multiple comparisons.

1. *performing neuronal activity measures, either via neural activity imaging or phospho-ERK labeling in different mutants at day or night conditions, to determine whether baseline neuronal activity brain-wide or in specific brain regions are altered.*

These are excellent experiments that we plan to perform in the future.

1. *Please check all Figure numbers for accuracy.*

We have double checked these.

1. *The authors emphasize the role of increased cellular sodium, but equally plausibly, the phenotypes could be due to decreased cellular potassium. The potassium channel shaker has been previously identified as a critical sleep regulator in Drosophila.*

We completely agree. We would like to highlight that we did devote an entire paragraph to the possibility of changes in extracellular potassium in the discussion: “A third possibility is that *Dmst* and the Na^+, K^+ -ATPase regulate sleep not by modulation of neuronal activity per se but rather via modulation of extracellular ion concentrations. Recent work has demonstrated that interstitial ions fluctuate across the sleep/wake cycle in mice. For example, extracellular K^+ is high during wakefulness, and cerebrospinal fluid containing the ion concentrations found during wakefulness directly applied to the brain can locally shift neuronal activity into wake-like states (Ding et al., 2016). Given that the Na^+, K^+ -ATPase actively exchanges Na^+ ions for K^+ , the high intracellular Na^+ levels we observe in *atp1a3a* and *dmst* mutants is likely accompanied by high extracellular K^+ . Although we can only speculate at this time, a model in which extracellular ions that accumulate during wakefulness and then directly signal onto sleep-regulatory neurons could provide a direct link between Na^+, K^+ ATPase activity, neuronal firing, and sleep homeostasis. Such a model could also explain why disruption of *fxyd1* in non-neuronal cells also leads to a reduction in night-time sleep.”

We also agree that Shaker may be an important component of this sleep regulatory mechanism. Indeed, we previously showed that another potassium channel in zebrafish regulates sleep (Rihel et al., 2010).

We have emphasized sodium homeostasis in our title and paper only because we were able to directly observe intracellular sodium levels, so we are confident that these have been altered in our mutants. We can only presume that potassium levels have also been altered, but we could not directly observe this.

1. *The similar phenotype between dmist and Fxyd1 in sleep reduction yet very different expression patterns, with dmist being mostly neuronal while fxyd1 being mostly non-neuronal, raise many possible questions: 1) are the sleep phenotypes due to neuronal Na/K imbalance? Or 2) Are the sleep phenotypes due to extracellular Na/K imbalance? Or 3) both? Some feasible experiments may help achieve a better mechanistic understanding of the observed sleep defects.*

Yes, we think these are excellent studies for future work. As noted in the previous point (20), we did discuss the possibility that changes to extracellular potassium might be a

parsimonious explanation for the similar phenotypes of fxyd1 and dmist mutants.

Future experiment suggestions (not required)

1. *Perform a double mutant analysis of fxyd1 and atp1a3a, to determine whether an epistatic relationship similar to that of dmist and atp1a3a is observed in the case of fxyd1 and atp1a3a.*

This is a great experiment that we will do in the future. Unfortunately, the fxyd1 mutant had been sperm frozen during the COVID-19 pandemic, so we cannot do this experiment at this time.

1. *Given the differences in the sleep phenotypes between vir/vir and i8/i8 mutants, would be informative to see the phenotype of the vir/i8 trans-heterozygote.*

This is also a good experiment to perform in the future. Since obtaining the cleaner i8 allele, the dmistvir/vir lines were sperm frozen.